Regulation of single inositol 1,4,5-trisphosphate receptor channel activity by protein kinase A phosphorylation

Larry E. Wagner II[1], Suresh K. Joseph[1] and David I. Yule[2]

[1] *Department of Pharmacology and Physiology, University of Rochester, 601 Elmwood Ave, Rochester, NY 14642, USA*
[2] *Department of Pathology, Anatomy and Cell Biology, Thomas Jefferson University, 230 Jefferson Alumni Hall, 1020 Locust Street, Philadelphia, PA 19107, USA*

Phosphorylation of inositol 1,4,5-trisphosphate receptors ($InsP_3R$) by PKA represents an important, common route for regulation of Ca^{2+} release. Following phosphorylation of the S2 splice variant of $InsP_3R$-1 (S2– InsP-1), Ca^{2+} release is markedly potentiated. In this study we utilize the plasma membrane (PM) expression of $InsP_3R$-1 and phosphorylation state mutant $InsP_3R$-1 to study how this regulation occurs at the single $InsP_3R$-1 channel level. DT40-3KO cells stably expressing rat S2– $InsP_3R$-1 were generated and studied in the whole-cell mode of the patch clamp technique. At hyperpolarized holding potentials, small numbers of unitary currents (average ∼1.7 per cell) were observed which were dependent on $InsP_3$ and the presence of functional $InsP_3R$-1, and regulated by both cytoplasmic Ca^{2+} and ATP. Raising cAMP markedly enhanced the open probability (P_o) of the $InsP_3R$-1 and induced bursting activity, characterized by extended periods of rapid channel openings and subsequent prolonged refractory periods. The activity, as measured by the P_o of the channel, of a non-phosphorylatable $InsP_3R$-1 construct (Ser1589Ala/Ser1755Ala $InsP_3R$-1) was markedly less than wild-type (WT) $InsP_3R$-1 and right shifted some ∼15-fold when the concentration dependency was compared to a phosphomimetic construct (Ser1589Glu/Ser1755Glu $InsP_3R$-1). No change in conductance of the channel was observed. This shift in apparent $InsP_3$ sensitivity occurred without a change in $InsP_3$ binding or Ca^{2+} dependency of activation or inactivation. Biophysical analysis indicated that channel activity can be described by three states: an open state, a long lived closed state which manifests itself as long interburst intervals, and a short-lived closed state. Bursting activity occurs as the channel shuttles rapidly between the open and short-lived closed state. The predominant effect of $InsP_3R$-1 phosphorylation is to increase the likelihood of extended bursting activity and thus markedly augment Ca^{2+} release. These analyses provide insight into the mechanism responsible for augmenting $InsP_3R$-1 channel activity following phosphorylation and moreover should be generally useful for further detailed investigation of the biophysical properties of $InsP_3R$.

(Received 8 February 2008; accepted after revision 3 June 2008; first published online 5 June 2008)
Corresponding author D. I. Yule: Department of Pathology, Anatomy, & Cell Biology, Thomas Jefferson University, 230 Jefferson Alumni Hall, 1020 Locust Street, Philadelphia, PA 19107, USA. Email: david_yule@urmc.rochester.edu

Three inositol 1,4,5-trisphosphate receptor ($InsP_3R$) genes code for distinct Ca^{2+} release channels of molecular mass ∼300 kDa, named $InsP_3R$-1, $InsP_3R$-2 and $InsP_3R$-3 (Furuichi *et al.* 1989; Sudhof *et al.* 1991; Maranto, 1994). Additional diversity is generated by alternative splicing of the $InsP_3R$-1 and $InsP_3R$-2 genes (Danoff *et al.* 1991; Iwai *et al.* 2005). $InsP_3R$-1 is the founding member of the family and was purified from cerebellum based on the abundance of the protein in this tissue (Supattapone *et al.* 1988*b*). In addition to the high relative expression level in cerebellum, this tissue is perhaps unique given that the $InsP_3R$-1 gene is expressed essentially in isolation in the Purkinje cells, whereas in other tissues the expression of multiple $InsP_3R$ types is the norm (Nakagawa *et al.* 1991; Wojcikiewicz, 1995; Taylor *et al.* 1999). The basic structural, biochemical and biophysical properties have also been defined largely based on the template of the $InsP_3R$-1 (reviewed in Foskett *et al.* 2007). For example, the domain structure of the receptors has been established in a linear array of ∼2700 amino acids as consisting of three general regions (Patel *et al.* 1999). Two major domains of high sequence homology between $InsP_3R$ types exist: the binding site for $InsP_3$ in the N-terminus (Yoshikawa

This paper has online supplemental material.

 DOI: 10.1113/jphysiol.2008.152314

et al. 1996), and a region in the C-terminus which constitutes the ion-conducting pore and determinants of tetramer formation (Galvan *et al.* 1999; Ramos-Franco *et al.* 1999; Joseph *et al.* 2000; Parker *et al.* 2004). The third domain, consisting of the intervening sequence, has been termed the 'regulatory and coupling domain' or 'modulatory' domain and is considerably more variable among $InsP_3R$ types. Regulation of Ca^{2+} release by factors such as Ca^{2+}, ATP, phosphorylation and interaction with protein binding partners occurs principally in this region (Berridge, 1993; Bezprozvanny & Ehrlich, 1993; Wojcikiewicz & Luo, 1998; Patel *et al.* 1999; Tang *et al.* 2003; Wagner *et al.* 2003, 2004; Bezprozvanny, 2005). One of the earliest forms of $InsP_3R$-1 regulation described was *via* phosphoregulation by protein kinase A (Supattapone *et al.* 1988*a*; Danoff *et al.* 1991). Indeed the protein was described as a phospho-protein prior to its identification as an intracellular Ca^{2+} release channel (Walaas *et al.* 1983, 1986). Phosphorylation of $InsP_3R$ by PKA serves as an important locus for cross-talk between two predominant, ubiquitous signal transduction pathways and has been suggested to play roles in such diverse Ca^{2+} regulated events as neural adaptation, epithelial cell fluid secretion and modulation of insulin secretion (Bruce *et al.* 2002, 2003; Tang *et al.* 2003; Chaloux *et al.* 2007). PKA activation results in stoichiometric phosphorylation of only two serine residues present in ideal predicted consensus motifs (RRXS) at Ser1589 and Ser 1755 in S2– $InsP_3R$-1 (Danoff *et al.* 1991; Soulsby *et al.* 2004). A series of studies from our laboratory have shown by measurement of $[Ca^{2+}]_i$ using fluorescent indicators that phosphorylation *per se*, or mimicking phosphorylation by introducing charge mutations at either residue, results in markedly enhanced $InsP_3$-induced Ca^{2+} release through S2– $InsP_3R$-1 (Wagner *et al.* 2003, 2004).

While these studies have unequivocally established which residues are functionally relevant for enhancing Ca^{2+} release through the $InsP_3R$-1, $[Ca^{2+}]_i$ measurements using fluorescent dyes as the functional readout are rather indirect and consequently provide limited mechanistic information regarding effects of phosphorylation on channel gating at the single $InsP_3R$ level. Indeed, in general, despite the important insight into $InsP_3R$ function provided by both biochemical studies and measurement of Ca^{2+} release, characterization of the electrophysiological and biophysical properties of the channel have lagged significantly. Until recently, the majority of studies of $InsP_3R$ function have been conducted following incorporation of $InsP_3R$ into planar lipid bilayers (Bezprozvanny *et al.* 1991; Bezprozvanny & Ehrlich, 1993; Ramos-Franco *et al.* 1998*a*,*b*). A general caution which complicates interpretation of bilayer data is that this preparation is likely to be missing regulatory input from the lipid environment as well as from protein binding partners and thus may not faithfully reflect the channel in its native environment.

Largely circumventing this issue, significant progress has been made by Foskett and colleagues studying $InsP_3R$ in the outer membrane leaflet of isolated nuclei using an 'on nucleus' configuration of the patch-clamp technique. This technique has yielded fundamental biophysical information regarding the gating and regulation of endogenous $InsP_3R$ in native membranes (Mak & Foskett, 1994, 1997; Stehno-Bittel *et al.* 1995; Mak *et al.* 1999, 2000, 2001, 2003; Boehning & Joseph, 2000; Boehning *et al.* 2001). A caveat which applies to both isolated nuclei and bilayer studies is that modulation from any endogenous cytosolic or PM input is necessarily absent and hence study of the regulation by endogenous signalling pathways is not generally possible.

Recently, a further methodological advance has been reported with the potential to significantly further our understanding of the electrophysiological and biophysical properties of $InsP_3R$. Surprisingly, it has been reported that a small number of $InsP_3Rs$ are resident in the PM of the chicken pre-B-lymphocyte cell line DT40. The limited PM expression permits the measurement of single $InsP_3R$ channel activity using the whole-cell mode of the patch-clamp technique (Dellis *et al.* 2006). Whether endogenously expressed in the wild-type DT40 cell, or stably expressed in a variant of the cell line where the native chicken receptors are ablated (DT40-3KO), one to four $InsP_3Rs$ are reliably present in the PM (Dellis *et al.* 2008). A particular utility of this system is the ability to express $InsP_3R$ and mutant constructs such that structure–function studies can be performed on an unambiguously $InsP_3R$ *null* background. In this system, the PM resident $InsP_3Rs$ are reported to be orientated such that the N and C termini retain their normal orientation in the cytoplasm and presumably are regulated in a relatively normal manner by cellular factors. This important attribute is, however, still to be established. The lipid environment of the receptor is also likely to be largely similar to the resident ER protein, although cholesterol and phospholipid levels may be somewhat greater in the PM than ER (Lange *et al.* 1999). Regulation by ER luminal factors will, however, clearly be absent. Important differences in activity may therefore be related to regulation by bath (luminal) Ca^{2+} and the absence of luminal accessory proteins such as the redox sensor ERp44 and chromagranin (Thrower *et al.* 2002; Higo *et al.* 2005). While the route of trafficking to the PM and the generality of this expression are at present unclear, the localization could provide an unprecedented opportunity to further define the key properties of $InsP_3Rs$ at the electrophysiological level.

Historically, there have been several studies describing PM resident $InsP_3R$ (Kuno & Gardner, 1987; Fadool & Ache, 1992; Vaca & Kunze, 1995; Tanimura *et al.*

2000; Kaur *et al.* 2001; Vazquez *et al.* 2002). It should be noted, however, that some of these reports have relied on characterization by indirect techniques and have subsequently not been substantiated. Thus, initially in this study we felt it imperative to validate the utility of this potentially important technique following stable expression of mammalian $InsP_3R$-1 constructs in DT40-3KO cells. We initially confirm that channel activity is $InsP_3R$-1 dependent and that the activity has characteristics shared with the receptor in its more conventional intracellular environment. The major focus of this work was then to investigate the modulation and regulation of gating of the $InsP_3R$-1 at the single channel level by PKA. Importantly, we demonstrate that PKA phosphorylation of S2– $InsP_3R$-1 increases the open probability of the $InsP_3R$-1 when the endogenous adenylate cyclase/PKA signalling pathway is activated by forskolin. By comparing the gating characteristics of non-phosphorylatable (S-A) mutations with phosphomimetic (S-E) mutations in the defined PKA phosphorylation sites, we show that PKA phosphorylation results in an increase in P_o of the $InsP_3R$-1. The increase in P_o primarily occurs by destabilizing a long lived closed state of the channel to facilitate bursting activity. This appears to take place by increasing the apparent affinity of the $InsP_3R$-1 for $InsP_3$ in the absence of marked effects of $InsP_3$ binding or modulation by cytosolic Ca^{2+}.

Methods

Electrophysiology

K^+ was utilized as the charge carrier in all experiments. In the majority of experiments intracellular free Ca^{2+} was clamped to favour activation of $InsP_3R$-1 unless otherwise stated (bath: 140 mM KCl, 10 mM Hepes, 500 μM BAPTA, free Ca^{2+} 250 nM, pH 7.1; pipette: 140 KCl, 10 mM Hepes, 100 μM BAPTA, 0.5 mM ATP, 200 nM free Ca^{2+}, pH 7.1). Pipette [Ca^{2+}] was calculated using MAXCHELATOR and verified by fluorimetry. The ATP was in the form of Na-ATP except in the *in vivo* phosphorylation experiments where Mg-ATP was included. Borosilicate glass pipettes were pulled and fire polished to resistances of about 20 MΩ. Following establishment of stable high resistance seals, the membrane patches were ruptured to form the whole-cell configuration with resistances > 5 GΩ and capacitances > 8 pF. The holding potential was set to -100 mV during the recording, except where noted, and currents were recorded under voltage clamp conditions using an Axopatch 200B amplifier and pCLAMP 9. Channel recordings were digitized at 20 kHz and filtered at 5 kHz with a -3 dB, 4-pole Bessel filter. Activity was typically evident 3–5 min after establishing the whole cell configuration at 1 μM $InsP_3$, but occurred essentially immediately following breakthrough with 100 μM $InsP_3$ in the pipette. In a similar fashion, channel activity occurred immediately when the pipette solution contained the high affinity $InsP_3R$ agonist, adenophostin A (ADO) (Adkins *et al.* 2000). A gravity fed multibarrelled glass perfusion pipette was used for local bath exchange during forskolin experiments.

Analyses were performed using the event detection protocol in Clampfit 9. Channel openings were detected by half-threshold crossing criteria. We assumed that the number of channels in any particular cell is represented by the maximum number of discrete stacked events observed during the experiment. All-points current amplitude histograms were generated from the current records and fitted with a normal Gaussian probability distribution function. The coefficient of determination (R^2) for every fit was > 0.95. The P_o was calculated using the multimodal distribution for the open and closed current levels. The effects on P_o of phosphorylation were calculated following 2 min of exposure to forskolin. Channel dwell time constants for the open and closed states were determined from exponential fits of all-points histograms of open and closed times from records appearing to contain one channel. The threshold for an open event was set at 50% of the maximum open current and events shorter than 0.1 ms were ignored. Closed times were only calculated for cells that contained one channel. A 'burst' was defined as a period of channel opening following a period of no channel activity which was greater than five times the mean closed time within a burst. The slope conductances were determined from the linear fits of the current–voltage relationships where $g = I_k/(V - V_k)$. Equation parameters were estimated using a non-linear, least squares algorithm. Two tailed heteroscedastic *t* tests with *P*-values < 0.05 were considered to have statistical significance. Ca^{2+} dependency curves were fitted separately for activation and inhibition with the logistic equation:

$$Y = \left[(A_1 - A_2)/\left(1 + (X/X_0)^P\right)\right] + A_2$$

Where A_1 is the minimal value, A_2 is the maximal value, X is the concentration of Ca^{2+}, X_0 is the half-maximal concentration and p is the slope related to the Hill coefficient.

Stable expression in DT40-3KO cells

Cell lines were created which stably express either wild-type (WT) S2– $InsP_3R$-1, a non-phosphorylatable construct in which the PKA phosphorylation sites at serine 1589 and serine 1755 were mutated to alanine (S2– $InsP_3R$-1S1589A/A1755A; henceforth termed 'AA') and a phosphomimetic construct in which these PKA phosphorylation sites were mutated to glutamate residues (S2– $InsP_3R$-1S1589E/S1755E; termed 'EE'). As previously

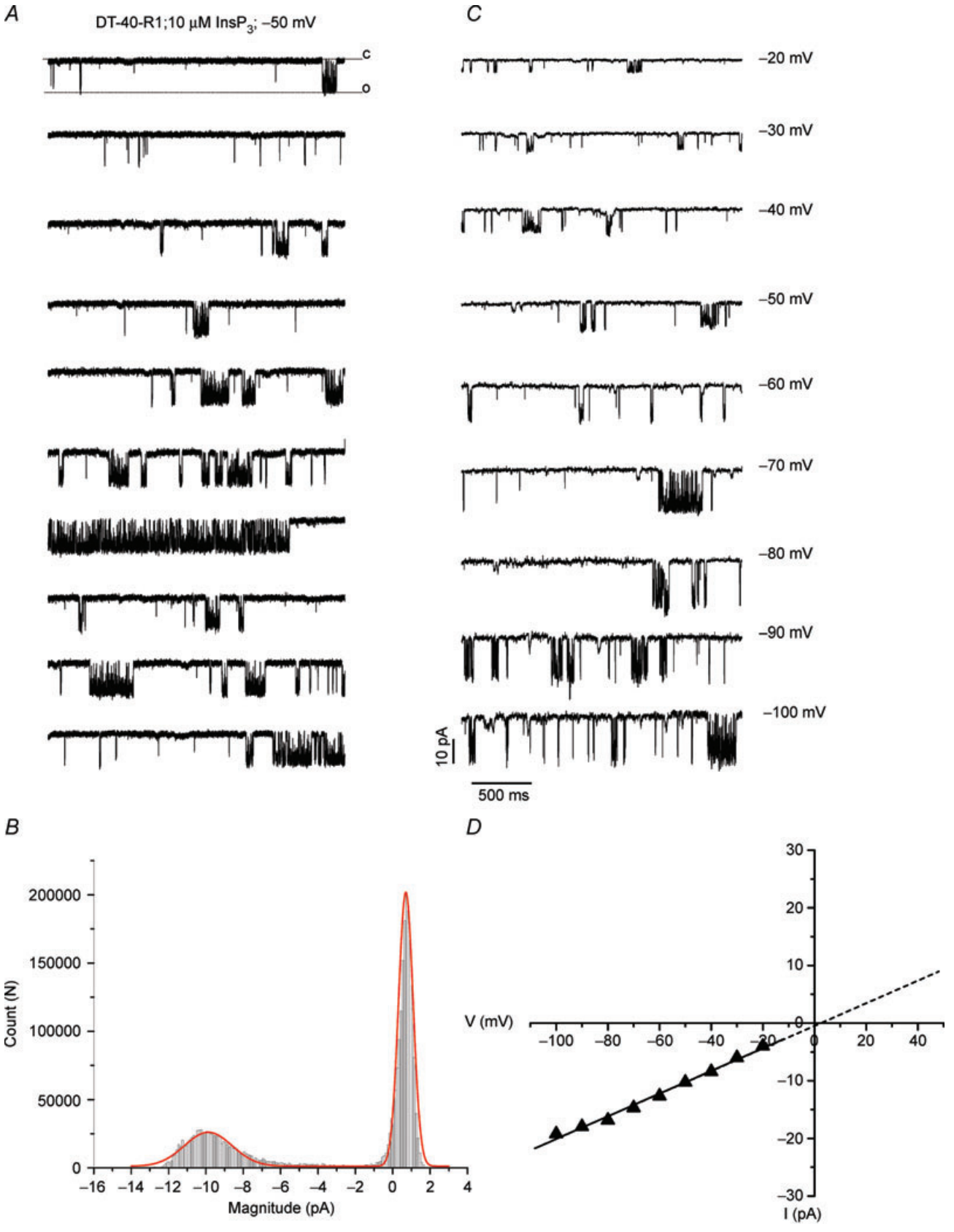

described (Wagner *et al.* 2006), *Nru*I digested plasmids were introduced into DT40 cells lacking expression of all $InsP_3R$ types (DT40-3K0 cells) by nucleofection using programme B23 and solution T as per the manufacturer's instructions (Amaxa, Inc., Gaithersburg, MD, USA). After nucleofection, the cells were incubated in growth media for 24 h prior to dilution in selection media containing 2 mg ml^{-1} geneticin (Invitrogen, Inc.). Cells were then seeded into 96-well tissue culture plates at approximately 1000 cells per well and incubated in selection media for at least 7 days. Wells exhibiting growth after the selection period were picked for expansion.

Binding assays

COS-7 cells were harvested by trypsinization, centrifuged at 150 *g* for 1 min and resuspended in HRB-HEDTA buffer containing 120 mM KCl, 20 mM Tris–Hepes (pH 7.2), 2 mM HEDTA and 1 mM PMSF, and permeabilized with saponin (10 μg mg^{-1} protein). A 0.8 ml aliquot of the permeabilized cells was incubated with 0.8 ml of a label mix containing 120 mM KCl, 20 mM Tris–Hepes (pH 7.2), 10 nM [^{3}H]IP_3 and different concentrations of unlabelled IP_3. After incubation on ice for 5 min, triplicate 0.5 ml samples were vacuum-filtered through A/E glass-fibre filters (Gelman Science, Ann Arbor, MI, USA), and the filters were washed with buffer containing 10 ml of 50 mM Tris-HCl (pH 7.8), 1 mM EDTA and 1 mg ml^{-1} bovine serum albumin. The filters were counted in Budget Solve (RPI, Mt Prospect, IL, USA) scintillation fluid. In order to normalize the binding measurements for variation in the expression of IP_3R constructs we always carried out transfections with WT $InsP_3R$-1 in parallel as a reference control. The expression of each of the constructs relative to the wild-type IP_3R was quantified densitometrically from immunoblots and used to calculate a factor (R) for the ratio of expression of the mutant relative to WT receptors. Normalized binding was obtained by dividing the binding values for each mutant by R. Control values are the mean ± S.E.M. of three independent experiments.

Results

Verification of $InsP_3R$-1 activity in DT40 cell PM

Initial experiments were performed to confirm that conditions could be established to unambiguously monitor single channel $InsP_3R$-1 activity in the PM of DT40-3KO cells stably expressing mammalian WT S2– $InsP_3R$-1. Unless otherwise indicated, all experiments were performed using S2– $InsP_3R$-1 or mutants constructed on this background. Following establishment of a high resistance seal (typically > 5 GΩ), the membrane patch was ruptured and the holding potential was maintained at 0 mV. Measurements were only continued in recordings with cellular capacitance of greater than 8 pF. Under these conditions, channel activity following pulses to negative potentials was entirely $InsP_3R$-1 dependent and was observed in > 90% of cells (see Fig. 2). In a minority of recordings, where the cellular capacitance recordings were under ∼4 pF, channel activity with a conductance of ∼190 pS was observed which was not dependent on $InsP_3$ or $InsP_3R$-1. The identity/localization of this channel is unknown but the low capacitance may reflect unmasking of $InsP_3$-independent channel activity following the formation of a bleb or intracellular vesicle after the attempt to achieve the whole cell configuration. A representative example of channel activity recorded with 10 μM $InsP_3$ in the patch pipette following pulses from 0 mV to −50 mV in WT DT40-3KO expressing $InsP_3R$-1 is shown in Fig. 1. Discrete single channel openings were observed punctuated intermittently by periods of bursting activity as shown in Fig. 1*A*. The average P_o was 0.3 ± 0.1 under these conditions. The high open probability during the bursts ($P_o > 0.8$) suggests that this particular experiment represents a cell with a single $InsP_3R$-1 present in the entire PM. In some cells, multiple channels were observed, but as previously reported (Dellis *et al.* 2006), never more than four channels were present. The average number of channels observed was 1.75 in 30 recordings of $InsP_3R$-1. Figure 1*B* shows the all-points current amplitude distribution for this particular cell at −50 mV for 102 concatenated sweeps. Little evidence of rundown was observed (> 5 min of acquisition) in any of these recordings. While a marked rundown in channel activity in *Xenopus* or Cos 7 cell nuclear patches has been reported, the PM $InsP_3R$-1 activity in DT40 cells appears similar to Sf9 cell nuclear patches where activity has been reported to be sustained over prolonged periods of time (Ionescu *et al.* 2006; Ionescu *et al.* 2007). The distribution illustrates a single major open state at a current amplitude of 10 pA with little evidence of obvious long lived subconductance states. Figure 1*C* shows representative

Figure 1. Channel activity in the PM of DT40 cells expressing $InsP_3R$-1
A, whole cell patch clamp recording of single channel $InsP_3R$-1 activity in an individual DT-40 cell stably expressing WT $InsP_3R$-1 using the standard recording solutions as described in Methods. Individual 3 s sweeps at −50 mV. C = closed; O = open state. *B*, all-points current amplitude histogram. Activity was detected using pCLAMP's event detection paradigm. Red trace shows bimodal Gaussian fit of the data. *C*, individual sweeps at the indicated potential. *D*, *I–V* relationship generated from the peak current amplitudes at each potential in C; the slope conductance is ∼200 pS.

sweeps acquired following pulses to increasing negative potentials and illustrates that as the driving force increases, the current amplitude similarly is larger. Figure 1*D* shows the current *versus* voltage (*I–V*) relationship for this channel generated from the peak K^+ conductance at each potential in Fig. 1*C*. At negative potentials, the *I–V* relationship behaved as an ohmic conductance and thus in symmetrical 140 mM K^+, the *I–V* relationship was linear with an extrapolated reversal potential at 0 mV (Fig. 1*D*). The *I–V* relationship revealed a calculated slope conductance of 202 ± 5 pS, a value close to that previously reported for $InsP_3R$-1 under these conditions (Dellis *et al.* 2006). The *I–V* relationship at positive potentials could not be resolved because of the presence of a large outwardly rectifying K^+ current seen even in the absence of $InsP_3$ and in DT-40-3KO cells as shown in Supplemental Fig. 1 (Dellis *et al.* 2006).

Next, experiments were performed to demonstrate that activation of $InsP_3R$-1 is responsible for the channel activity observed. For these experiments the high affinity $InsP_3R$ agonist ADO was used because like saturating [$InsP_3$], no delay in the initiation of activity was seen following breakthrough. This characteristic was deemed important for an accurate appreciation of mean P_o for comparison in later experiments where lower levels of $InsP_3R$-1 stimulation were tested. Each panel in Fig. 2 shows single representative sweeps from multiple cells for a particular condition in which a recording was maintained for greater than 5 min. Figure 2*A* demonstrates that in the absence of ADO, no activity is observed in cells stably expressing $InsP_3R$-1 ($n = 5$ cells, total recorded time > 20 min). In contrast, activity was always evident under otherwise identical conditions but in the presence of ADO (Fig. 2*B*; $n = 5$). Note that in the examples shown, clear evidence of stacking events, i.e. the activity of multiple channels, was observed. These data clearly indicate the dependence on the presence of $InsP_3R$ agonist for the channel activity. In DT-40-3KO cells (in the absence of $InsP_3R$), ADO failed to stimulate channel activity (Fig. 2*C*, $n = 5$, total recording time > 40 min). Similarly, in the presence of heparin, an $InsP_3R$ antagonist, ADO also failed to initiate channel activity (Fig. 2*D*; $n = 5$, total recording time > 20 min). Channel activity was also refractory in a cell stably expressing a mutant of S2+ $InsP_3R$-1, which is expressed normally and binds $InsP_3$ but which under these conditions (Ca^{2+} present; K^+ as the charge carrier) is rendered 'pore-dead' by a mutation in a residue lining the putative conduction pathway (Boehning & Joseph, 2000; Boehning *et al.* 2001; van Rossum *et al.* 2004) (Fig. 2*E*, $n = 12$, total recording time > 60 min). This mutatant has been reported to conduct K^+ in the absence of Ca^{2+} (Dellis *et al.* 2008). In our hands, with bath [Ca^{2+}] reduced to < 10 nM similarly no channel activity was observed (data not shown). In total these data provide substantial evidence that functional $InsP_3R$-1 is necessary for the channel activity seen. Although, the recording conditions are such that intracellular Ca^{2+} is relatively well buffered, it is formally possible that the activity observed is a consequence of $InsP_3$-induced Ca^{2+} release, i.e. a Ca^{2+} activated conductance, rather than a direct assay of the $InsP_3R$-1 itself. Similar activity was, however, observed when intracellular buffering was considerably more stringent as the [BAPTA] was increased to 5 mM (data not shown). Perhaps most compelling, experiments were also performed recording activity from cells stably expressing a construct which has a mutation in the ion conducting pore. This mutation results in rational and documented changes in the characteristics of the conductance. Specifically, when the valine present in the putative pore of the S2+ $InsP_3R$-1 is mutated to isoleucine, the corresponding amino acid present in the RYR, a channel with similar selectivity but higher conductance, has been observed (Boehning *et al.* 2001). As predicted, expression of this construct resulted in a current of larger single channel amplitude (Fig. 2*F*, $n = 4$). The all-points amplitude for events recorded at -50 mV shows a distribution for the V2548I mutant left shifted to centre around 13.3 pA. The slope conductance generated from the *I–V* relationship shows an increased conductance of 266 ± 8 pS *versus* 202 ± 5 pS for the WT $InsP_3R$-1 activated by ADO. Because these mutations directly modify the core biophysical properties of the $InsP_3R$-1 in a predictable manner, they provide considerable strength to the argument that these data reflect direct measurement of the $InsP_3R$-1 single channel activity.

Regulation of PM $InsP_3R$-1 activity by Ca^{2+} and ATP

$InsP_3R$-1 activity, whether monitored in the ER or reconstituted in bilayers, is well documented to be regulated in a predicable manner by both cytosolic Ca^{2+} and ATP (Iino, 1990, 1991; Bezprozvanny *et al.* 1991; Finch *et al.* 1991; Bezprozvanny & Ehrlich, 1993). To further strengthen the contention that channel activity observed in these recordings is a result of $InsP_3R$-1 activity and importantly that the channel behaves in an appropriate fashion, preliminary experiments were performed to characterize both the Ca^{2+} and ATP dependence of PM channel activity. The pipette solution contained an activating concentration of ADO and the [Ca^{2+}] as indicated. As shown in Fig. 3*A* and summarized in Fig. 3*B*, the channel activity was enhanced as the [Ca^{2+}] was increased in the pipette solution. Under these conditions, maximal channel activity was achieved with ~ 200 nM Ca^{2+} (EC_{50} for activation $k_{act} = 97 \pm 15$ nM). Consistent with other reports, at [Ca^{2+}] greater than 1 μM channel activity subsequently decreased (EC_{50} for inhibition $k_{inh} = 4.1 \pm 0.6$ μM). A further characteristic mode of regulation of $InsP_3R$-1 activity is through

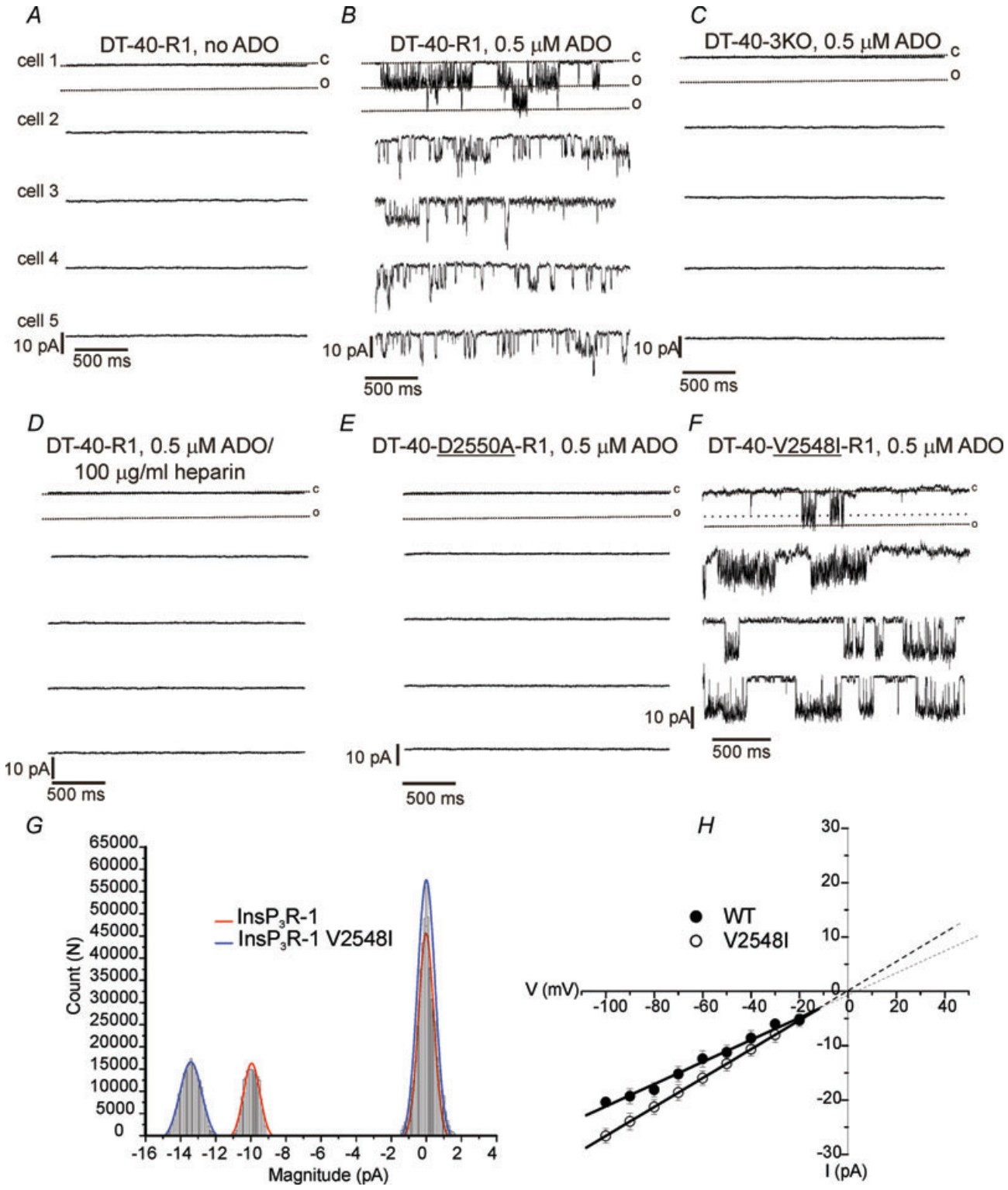

Figure 2. Verification of $InsP_3R$-1 dependent channel activity
A–F, single sweeps from multiple cells following a pulse to −50 mV. *A*, recording from WT $InsP_3R$-1 in the absence of ADO. *B*, presence of ADO. *C*, DT40-3KO cells ($InsP_3R$ *null* cells). *D*, ADO in the presence of the $InsP_3R$ antagonist heparin. *E*, from a stable DT40-3KO cell line expressing S2+ splice variant D2550A $InsP_3R$-1, a 'pore-dead' mutant $InsP_3R$-1. *F*, from a stable DT40-3KO cell-line expressing S2+ splice variant V2548I $InsP_3R$-1, a mutation in a residue in the putative pore of $InsP_3R$-1 which corresponds to the residue present in ryanodine receptors. *G*, all-points amplitude histogram; red and blue traces are Gaussian fits of the data. *H*, *I–V* relationship for the WT and V2548I $InsP_3R$-1.

allosteric modulation by cytosolic ATP (Iino, 1991; Bezprozvanny & Ehrlich, 1993; Mak *et al.* 1999; Maes *et al.* 2000, 2001). Figure 4*A* (individual traces) and Fig. 4*B* (pooled data) clearly show that at 0.5 μM ADO and activating [Ca^{2+}] (200 nM) increasing [ATP] results in an increased $InsP_3R$-1 P_o. In total, these data strongly suggest that whole-cell channel activity observed is the result of ectopically expressed mammalian $InsP_3R$-1 localized in the PM. Importantly, key characteristics and fundamental regulatory inputs of $InsP_3R$-1 activity are retained in this environment.

Regulation of $InsP_3R$-1 following PKA activation

Regulation of $InsP_3R$-1 channel activity in bilayers has been monitored following addition of catalytic subunits of PKA (Tang *et al.* 2003). However, because elements of the signalling cascade are absent, regulation following

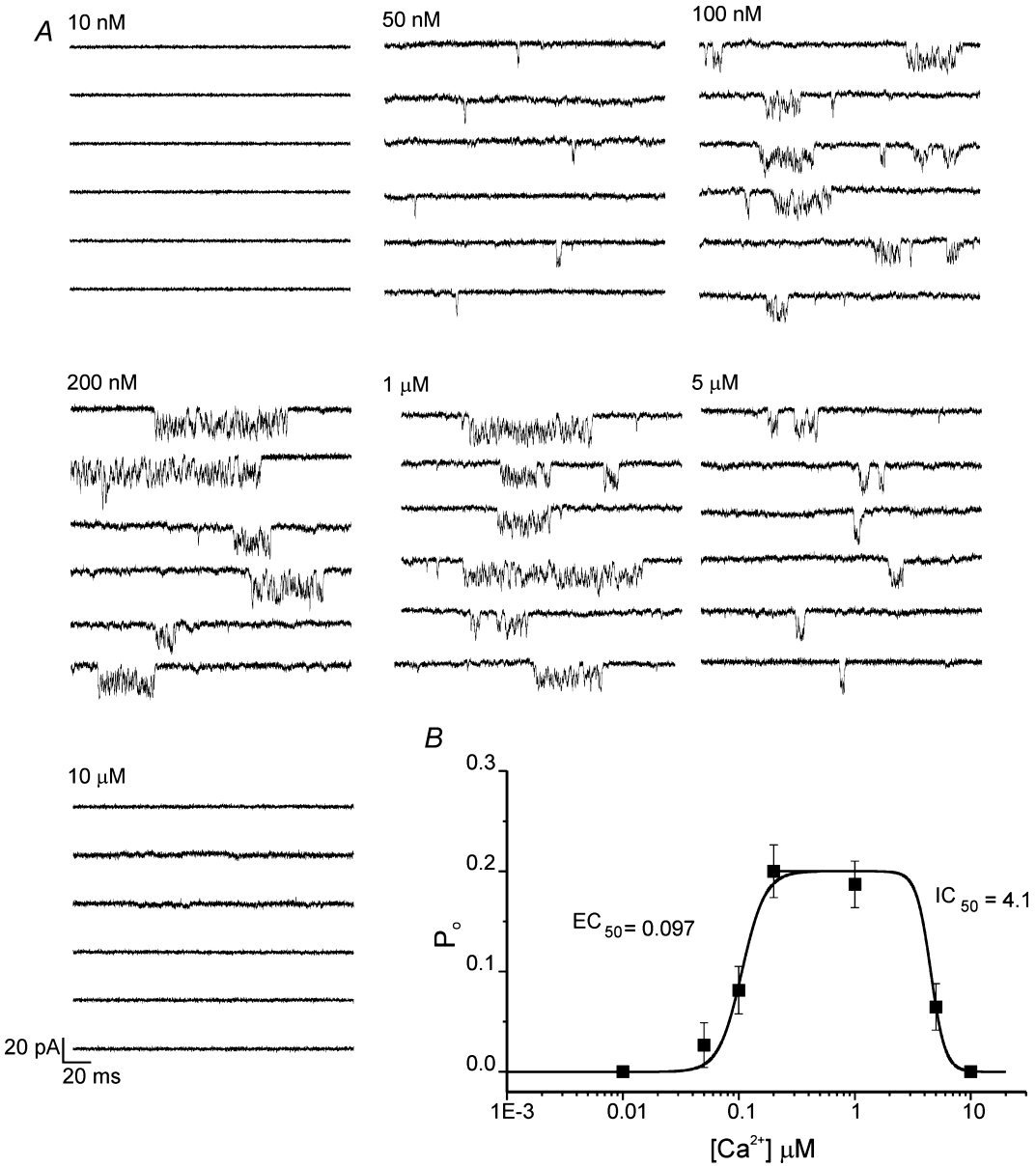

Figure 3. Cytosolic Ca^{2+} dependency of $InsP_3R$-1 activity
A, pairs of representative 500 ms sweeps recorded at −100 mV at the indicated intracellular [Ca^{2+}] and 0.5 μM ADO. Traces are shown from 3 cells under each condition. Channel activity is absent at 10 nM Ca^{2+}, but activity increases as the [Ca^{2+}] is increased. Maximal open probability occurs at ∼200 nM Ca^{2+}. At concentrations greater than 1 μM, the activity is reduced and is again absent at [Ca^{2+}] > 5 μM. *B*, the Hill equation fits of the pooled data ($n > 5$, for each [Ca^{2+}]).

activation of endogenous pathways is unlikely to be observable in bilayers or in nuclear patches. The measurement of PM $InsP_3R$-1 activity by whole cell patch clamp provides a unique opportunity to monitor the dynamic regulation of the channel following the activation of adenylate cyclase and appropriately targeted PKA. Channels were activated under whole-cell recording conditions with a pipette solution containing 0.5 μM ADO, activating [Ca^{2+}] and [ATP] (200 nM and 0.5 mM, respectively). After establishing a stable recording, cells were exposed to 20 μM forskolin by superfusion *via* a pipette placed close to the patch-clamped cell. As shown in Fig. 5*A* (individual representative sweeps from one cell at the times indicated, typical of 5 experiments) and Fig. 5*B* (cumulative plot), following incubation with forskolin, the mean $InsP_3R$-1 P_o markedly increased. No channel activity was observed following forskolin exposure in DT40-3KO (absence of $InsP_3R$). These data are consistent with the reported effects of addition of catalytic PKA subunits to S2+ $InsP_3R$-1 incorporated in lipid bilayers (Tang *et al.* 2003). $InsP_3R$-1 activity during forskolin treatment appeared to alter the predominant gating mode of the channel as activity was characterized by more extended episodes of 'bursting activity' during which the $InsP_3R$-1 exhibited very high P_o for extended periods of time followed by periods when channel opening was refractory. Of note, exposure to forskolin and the resultant marked increase in P_o never resulted in the obvious appearance of stacking events, as evidence of additional $InsP_3R$-1 in the PM (mean channel number ~1.7 before and after forskolin treatment). Following washout of forskolin, the channel P_o returned towards basal values.

Electrophysiological characterization of phosphomimetic and non-phosphorylatable $InsP_3R$-1 constructs

Several factors complicate the analysis of $InsP_3R$-1 activity following PKA activation. First, phosphorylation and subsequent dephosphorylation are dynamic events and

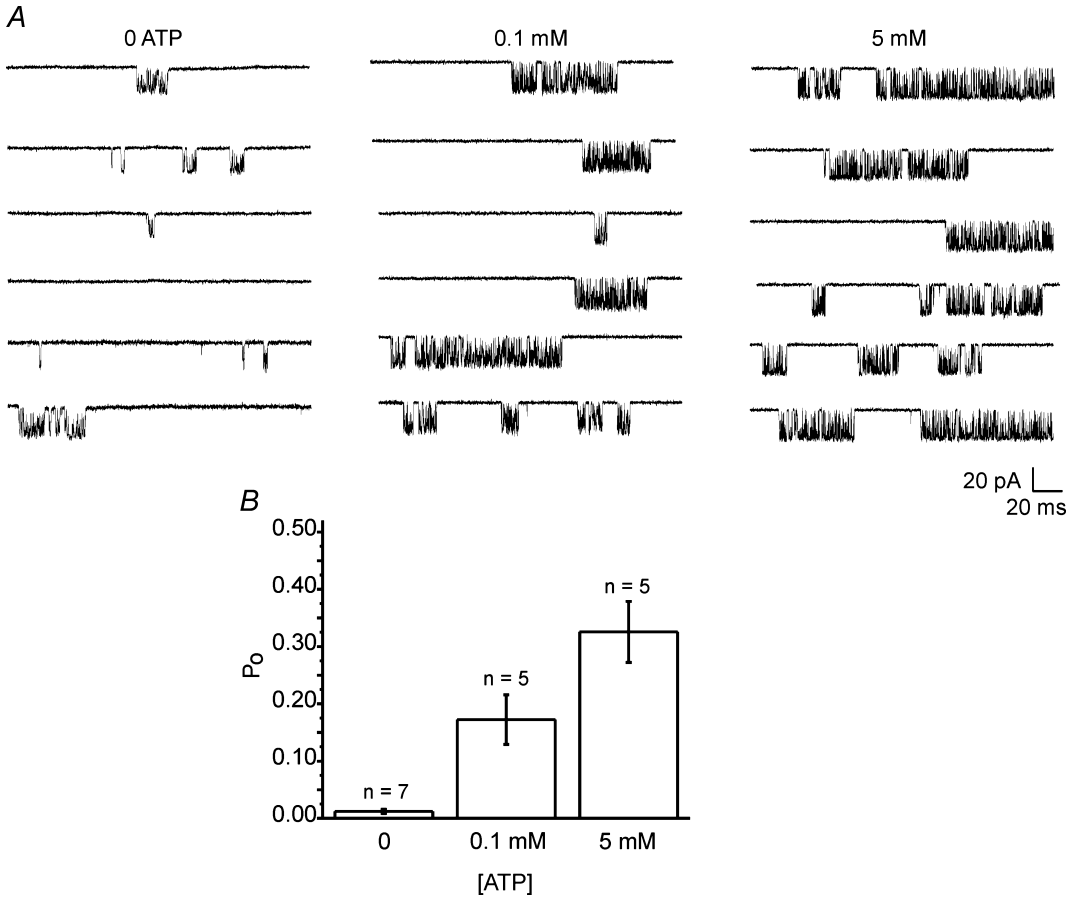

Figure 4. Cytosolic ATP dependency of $InsP_3R$-1 activity
A, pairs of representative 500 ms sweeps recorded at −100 mV at the indicated intracellular [ATP]. The pipette recording solution contained 0.5 μM ADO and 200 nM Ca^{2+}. Traces are shown from 3 cells under each condition. Channel activity is enhanced as the [ATP] is increased. *B*, pooled data.

thus the observed activity cannot be considered to be at steady-state. Second, phosphorylation of individual sites could occur in a cell type specific manner as a result of targeting. Third, raising cAMP will result in phosphorylation of numerous additional substrates which could conceivably affect channel activity. Furthermore, a degree of constitutive phosphorylation may occur which may attenuate the observed effects (Wagner *et al.* 2006). To circumvent these issues, we next chose to study the electrophysiological characteristics of phosphorylation state mutant $InsP_3R$-1. The rationale was that an analysis of the behaviour of these channels would provide

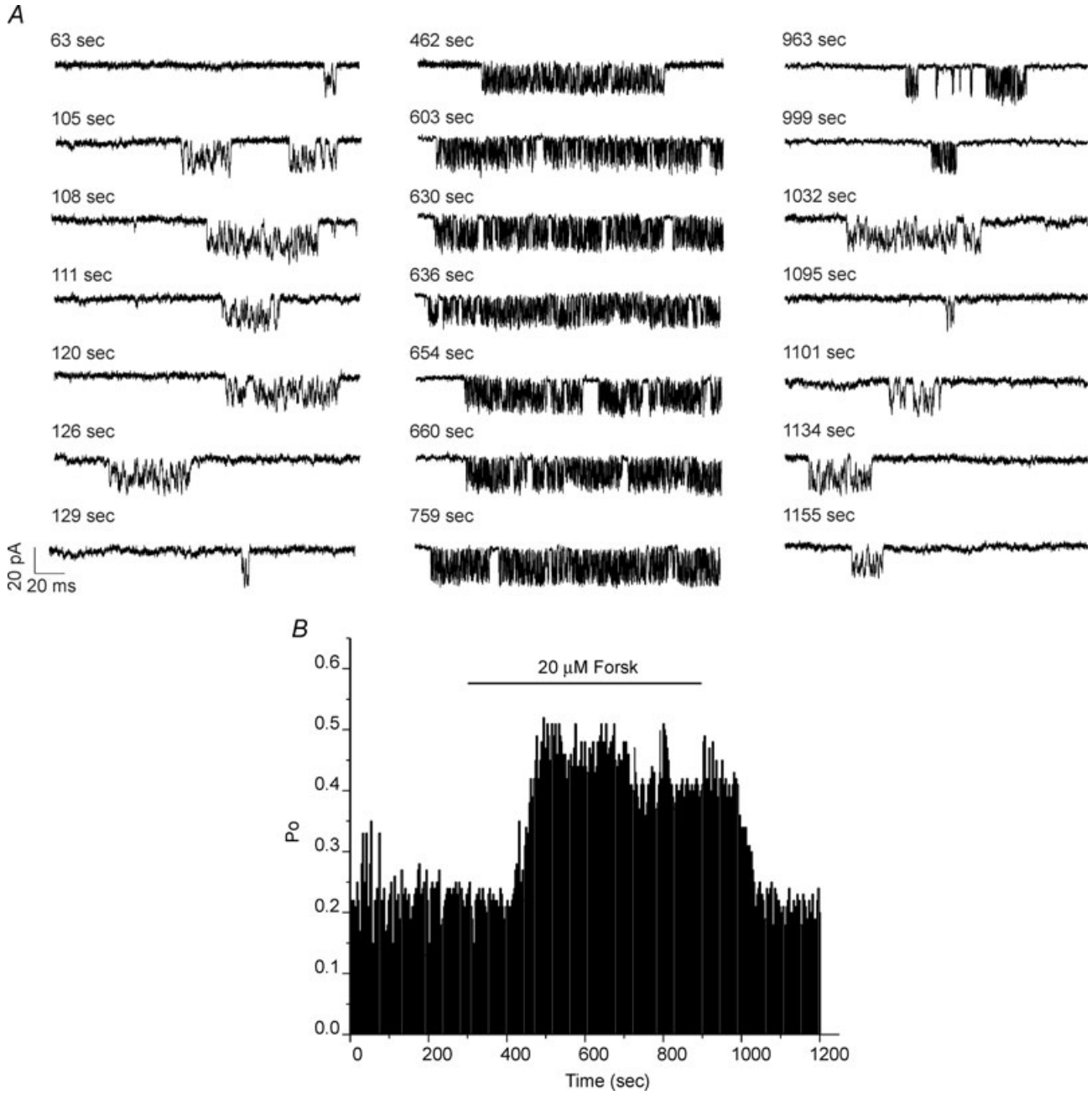

Figure 5. Forskolin enhances $InsP_3R$-1 channel activity
A, representative sweeps at −100 mV from an individual cell at the indicated time points. The left panel is sweeps before forskolin application, the middle panel is sweeps during forskolin application to activate adenylate cyclase and PKA, and the right panel contains sweeps after wash-out of the forskolin. *B*, a diary plot of the P_o *versus* time, demonstrating that activation of adenylate cyclase markedly enhances P_o *versus* channel activity prior to stimulation ($P = 0.0012$).

powerful tools to glean mechanistic insight into the effects of PKA phosphorylation of $InsP_3R$-1. We have previously documented that substitution of the serine residues in the phosphorylation sites with glutamate, presumably by virtue of the change in charge, mimics the characteristics of phosphorylation (EE $InsP_3R$-1), while substitution with alanine at these sites renders the $InsP_3R$-1 non-phosphorylatable (AA $InsP_3R$-1) (Wagner *et al.* 2003, 2004). Figure 6 shows representative sweeps from multiple cells stably expressing either AA $InsP_3R$-1 (Fig. 6*A*) or EE $InsP_3R$-1 (Fig. 6*B*) and exposed to a pipette solution identical to that used in Fig. 5 (0.5 μM ADO, 200 nM Ca^{2+} and 0.5 mM ATP). The *I–V* relationships and slope conductances derived for AA and EE $InsP_3R$-1 were indistinguishable from WT $InsP_3R$-1 indicating that the mutation did not alter the conductance of the channel (Fig. 6*D*). The average number of channels observed in cells expressing these constructs was not different when compared to WT $InsP_3R$-1, consistent with phosphorylation not increasing the absolute number of channels at the PM (1.74 for EE, 171 cells; and 1.78 for AA, 23 cells). Single channel activity in AA $InsP_3R$-1 was characterized by sparse, brief openings resulting in a low mean P_o of 0.01 ± 0.02. This low mean P_o of AA $InsP_3R$-1 compared to WT $InsP_3R$-1 at this [ADO] is consistent with our previous interpretation that WT

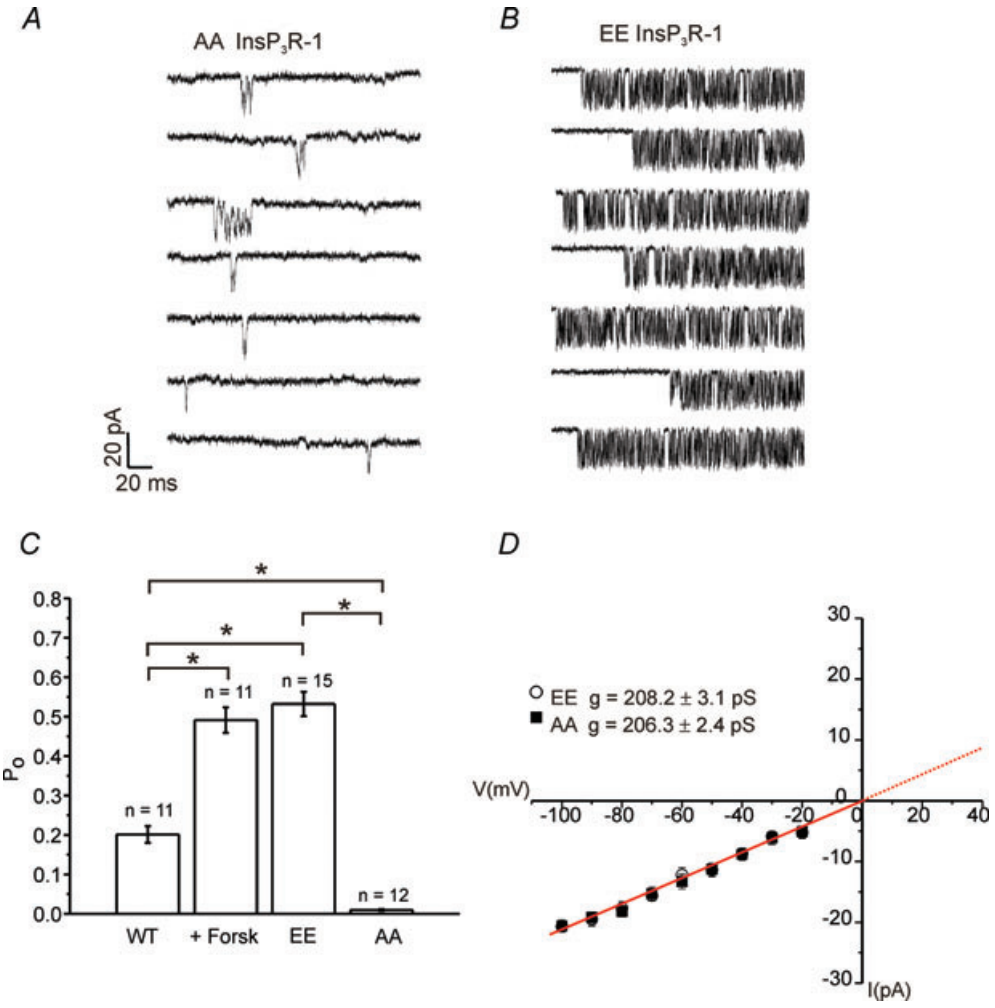

Figure 6. Comparison of phosphorylation state mutant $InsP_3R$-1 constructs
A, representative sweeps at −100 mV from individual cells expressing AA $InsP_3R$-1, a mutant $InsP_3R$-1 which cannot be phosphorylated by PKA. The pipette solution contained 500 nM ADO–0.5 mM ATP–200 nM Ca^{2+}. *B*, representative sweeps from individual cells expressing EE $InsP_3R$-1, a mutant $InsP_3R$-1 which by virtue of charge largely mimics phosphorylation by PKA. Channel activity is greater in the EE $InsP_3R$-1 *versus* AA $InsP_3R$-1 and WT $InsP_3R$-1 under identical conditions ($P = 0.001$ EE *versus* AA; $P = 0.001$ WT *versus* EE). WT $InsP_3R$-1 exhibits significantly higher P_o than AA $InsP_3R$-1 ($P = 0.001$). *C*, pooled data; asterisks indicate statistical significance. *D*, the *I–V* relationship for AA and EE $InsP_3R$-1. The slope conductances derived from these data show that the conductance of these constructs are very similar and not different from WT $InsP_3R$-1 (see Fig. 1).

$InsP_3R$-1 is likely to be, at least partially, constitutively phosphorylated under basal conditions (Wagner *et al.* 2006). In contrast, activation of EE $InsP_3R$-1 resulted in a channel exhibiting a high mean P_o of 0.53 ± 0.03 and extended periods of bursting activity which was comparable to the activity observed for WT $InsP_3R$-1 exposed to forskolin (Fig. 6*C*). The activity of AA or EE $InsP_3R$-1 was unaffected by treatment with forskolin (AA P_o following forskolin 0.01 ± 0.01 ($n = 4$); EE P_o following forskolin 0.44 ± 0.07 ($n = 4$)), presumably because, as expected, no further functionally important PKA phosphorylation sites are amenable to regulation in these construct (Wagner *et al.* 2003, 2004; Soulsby *et al.* 2004).

Phosphorylation alters the functional affinity of $InsP_3R$-1 but does not affect binding of $InsP_3$

Next, channel activities of AA $InsP_3R$-1 and EE $InsP_3R$-1 were compared over a range of [ADO]. As shown in Fig. 7*B*, channel activity was readily evident at 20 nM ADO in EE $InsP_3R$-1 and reached a maximal P_o at $\sim 0.5\ \mu$M. AA $InsP_3R$-1 was refractory to ADO until much higher concentrations and the maximum P_o was not reached until $10\ \mu$M ADO (Fig. 7*A*). Indeed, the EC_{50} was left shifted some 15-fold from 2495 ± 52.2 nM to 168.5 ± 28.1 nM when comparing AA to EE $InsP_3R$-1 (Fig. 7*C*). Of note, the maximum achievable P_o was comparable for both phosphorylation state mutants and the tendency of each mutant to exhibit bursting activity increased with [ADO]. These data indicate that phosphoregulation of $InsP_3R$-1 appears to increase the functional affinity of the receptor for $InsP_3$. This observation could be simply explained by an increased $InsP_3$ affinity for the PKA phosphorylated $InsP_3R$-1. To test this idea, we performed radioligand competition assays in permeabilized Cos-7 cells transiently expressing $InsP_3R$-1 constructs. This experimental system was chosen as a convenient screen based on high transfection efficiency, and low endogenous levels of $InsP_3R$ (Boehning *et al.* 2001). As shown in Fig. 8, while [^{3}H]$InsP_3$ binding could be readily measured for each construct although slightly lower in AA and EE, the relative affinity of the $InsP_3R$-1 did not appear to be markedly altered when comparing WT, AA and EE $InsP_3R$-1 (Fig. 8). Thus, an alteration in $InsP_3$ binding *per se* does not appear to account for the increased apparent functional sensitivity of the $InsP_3R$-1 following PKA phosphorylation. These data are consistent with an earlier study which reported the absence of any effect of incubation with PKA catalytic subunit on [^{3}H]$InsP_3$ binding to cerebellar microsomes (Supattapone *et al.* 1988*a*).

Phosphorylation does not alter Ca^{2+} activation or deactivation of the $InsP_3R$-1

Ca^{2+} acts as a coagonist at the $InsP_3R$ and is undoubtedly the most important regulator of $InsP_3R$ function. In the absence of a modulatory effect of phosphorylation on $InsP_3$ binding, we investigated if the mechanism underlying the effect of PKA phosphorylation was to alter the tuning of the $InsP_3R$ by Ca^{2+} to favour release. Channel activity was monitored in either AA $InsP_3R$-1 or EE $InsP_3R$-1 with a pipette solution containing $0.5\ \mu$M ADO, 0.5 mM ATP and Ca^{2+} varied between 10 nM and $10\ \mu$M. The concentration of ADO was chosen to maximally stimulate the EE construct. Because of the differing apparent affinity of $InsP_3$ for the phosphorylated *versus* non-phosphorylated receptor the protocol should reveal any [$InsP_3$]-dependent differences in activity. $InsP_3R$-1 activity followed the characteristic biphasic relationship for both mutant constructs. Channel activity was essentially absent when pipette Ca^{2+} was buffered to below what is considered resting cytosolic values ($\sim$50 nM) and increased to maximal activity between 200 nM and $1\ \mu$M. Although the absolute P_o was lower in AA $InsP_3R$-1, when the open-probability was normalized to each construct's maximum P_o, essentially identical EC_{50} values were derived from the Hill equation fits for the Ca^{2+} effect on activation of $InsP_3R$-1 activity in AA, EE and WT $InsP_3R$-1 as shown in Fig. 9 (k_{act} (nM) $= 97 \pm 15$, WT; 114 ± 17, EE; and 110 ± 14, AA. Similarly, no difference was observed for the inhibition of $InsP_3R$-1 activity (k_{inh} (μM) $= 4.1 \pm 0.2$, WT; 4.3 ± 0.1, EE; 4.1 ± 0.2, AA.

Analysis of the gating characteristics of phosphorylated $InsP_3R$-1

A prominent feature of the $InsP_3R$-1 activity is the tendency of the channel to exhibit bursting activity characterized by periods of high P_o followed by extended refractory periods. The biophysical basis for the increase in P_o following phosphorylation was explored by analysing the open and closed time distributions from within bursts. First, the distribution of open dwell times for AA $InsP_3R$-1, EE $InsP_3R$-1 and WT $InsP_3R$-1 in the presence and absence of forskolin were analysed. The distributions were well described by a single exponential fit, indicating a single predominant open state for each construct. The mean open-times for each construct/condition were very similar (WT $InsP_3R$-1, 0.3 ± 0.04 ms; WT + forskolin, 0.3 ± 0.03 ms; EE $InsP_3R$-1, 0.3 ± 0.03 ms; AA $InsP_3R$-1, 0.3 ± 0.03 ms). The time constant (τ) calculated from these fits was not significantly altered either in the mutants or following treatment of WT $InsP_3R$-1 with forskolin. These data indicate that the principal effect of phosphorylation is not to alter the transition from the open to this closed state during the bursts (Fig. 10). The

distribution of closed times within a burst was analysed and was again well described by a single exponential. A detailed description of the closed time distribution for AA $InsP_3$R-1 was not obtained because the low P_o of the channel under these conditions made ascertaining the absolute number of channels present problematic. Nevertheless, within the bursts the mean closed time of AA $InsP_3$R-1 appeared similar to WT. Analysis of

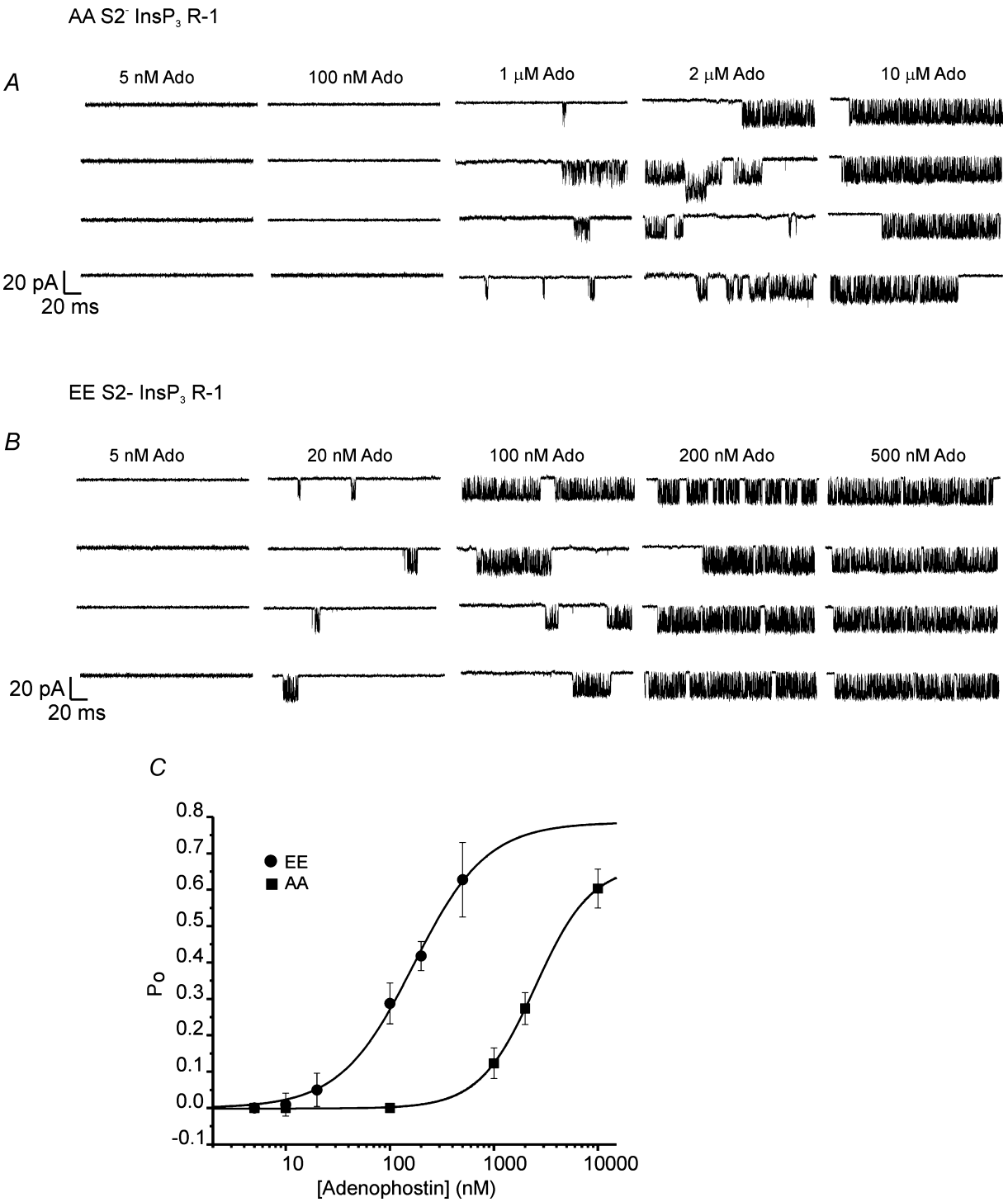

Figure 7. Functional sensitivity of phosphorylation state mutant $InsP_3$R-1 constructs
A, representative records from individual AA $InsP_3$R-1 expressing cells at the indicated [ADO] and a pipette solution containing 200 nM Ca^{2+} and 0.5 mM ATP. *B*, representative sweeps under identical conditions to *A* in cells expressing EE $InsP_3$R-1. *C*, concentration–response relationships from pooled data ($n > 5$ for each [ADO]). The functional sensitivity of AA $InsP_3$R-1 is ∼15-fold lower than EE $InsP_3$R-1.

the closed time distributions of the remaining $InsP_3R$-1 constructs indicated that the τ decreased modestly, but significantly when comparing WT $InsP_3R$-1 to receptor following treatment with forskolin or when comparing WT to the EE $InsP_3R$-1 (Fig. 11). These data indicate that an effect of PKA phosphorylation of $InsP_3R$-1 is the destabilization of this short-lived intraburst closed state of the channel, leading to an increase in open-probability within the burst.

The presence of long interburst intervals indicates that the channel also appears to reside in additional much longer-lived closed state(s). We next examined the bursting behaviour of AA and EE $InsP_3R$-1 by analysing 35 min of concatenated traces for each construct. The initiation of a burst was defined as a period, prior to activity, of at least 5 times the mean closed time within a burst for each individual construct and consisting of at least two openings. Conversely, the termination of a burst was characterized by a further period of closed time equal to, or greater than, 5 times the mean closed time in a burst. The mean WT closed time was used to define the minimal interburst interval for AA $InsP_3R$-1 (mean closed times: WT $InsP_3R$-1, 0.6 ± 0.03 ms; EE $InsP_3R$-1, 0.4 ± 0.03 ms). The distribution of burst lengths for both constructs was well described by a single exponential. The τ for EE was significantly longer than for AA (Fig. 12*A* and *B*, EE and AA, respectively) indicating that phosphorylation markedly decreases the rate of transition into the longer-lived closed state. Analysis performed on WT $InsP_3R$-1 before and during forskolin treatment showed a similar increase in τ from 19.3 ± 0.9 to 97.6 ± 3.4 ms following PKA phosphorylation. Examination of the distribution of the interburst intervals also revealed a dramatic decrease in the τ for EE $InsP_3R$-1 when compared to AA $InsP_3R$-1 (Fig. 12*C* and *D*, EE and AA, respectively).

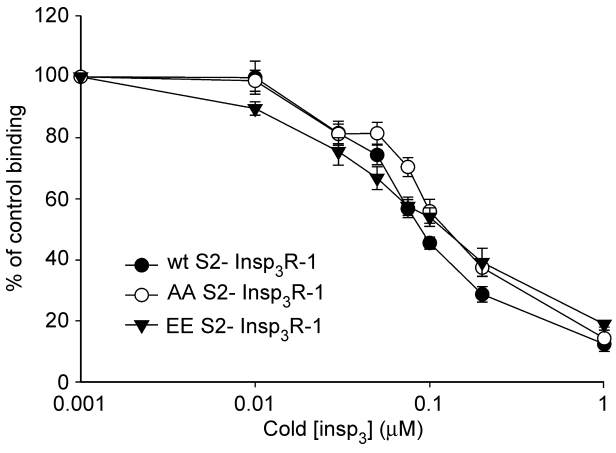

Figure 8. Binding of $InsP_3$ to AA and EE $InsP_3R$-1 is equivalent
Binding of [^{3}H]$InsP_3$ to permeabilized Cos 7 cells transiently expressing the indicated constructs. The affinity of EE, AA and WT $InsP_3R$-1 are not significantly different.

This observation would therefore suggest that, in addition to decreasing the rate of transition into a long-lived closed state, phosphorylation of the channel markedly accelerates the transition out of the long-lived closed state prior to bursting. A similar decrease in τ was observed when comparing the distribution of interburst intervals for WT $InsP_3R$-1 following forskolin treatment ($\tau = 63.8 \pm 2.1$ *versus* 6.7 ± 1.7 ms, WT $InsP_3R$-1 and forskolin treated, respectively), consistent with the idea that the phosphomimetic constructs are an appropriate surrogate for studying native phosphoregulation.

Discussion

The ability to express $InsP_3R$ constructs and mutants on an unambiguously null background and study their single channel characteristics is a powerful tool with the potential to provide considerable insight into structure–function relationships and the regulation of $InsP_3R$ in a native lipid environment. As a pivotal first step in this study, we have provided strong evidence that unitary PM $InsP_3R$-1 activity can be readily measured using whole cell patch clamp of DT4O cells. These experiments essentially verify and further expand on the initial characterization by Taylor and colleagues, who proposed a role for the PM localized $InsP_3R$ in mediating stimulated Ca^{2+} influx in lymphocytes (Dellis *et al.* 2006). The primary evidence

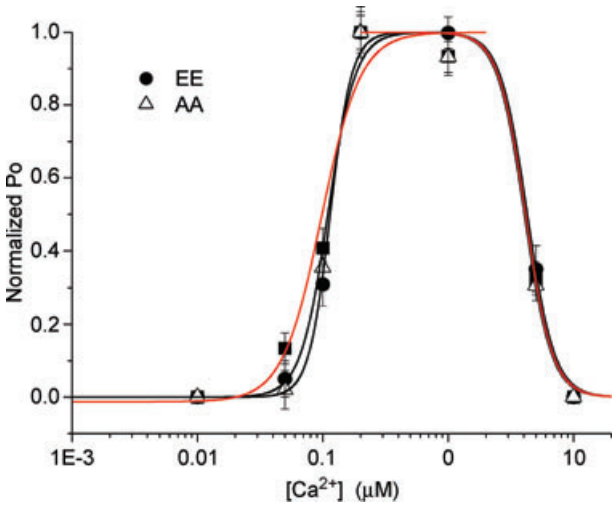

Figure 9. Cytosolic Ca^{2+} dependency of phosphorylation state mutant $InsP_3R$-1 constructs
Pooled data from cells expressing AA or EE $InsP_3R$-1 at the [Ca^{2+}] indicated and a pipette solution containing 0.5 μM ADO and 0.5 mM ATP. The P_o was normalized to the maximal P_o for each construct ($n > 5$ for each [Ca^{2+}]). The black curves are the Hill equation fits of the AA and EE $InsP_3R$-1 data. The red curve represents the Hill equation fit of the WT $InsP_3R$-1 data reproduced from Fig. 3. The Ca^{2+} dependency for the activation or inhibition of $InsP_3R$-1 activity was not significantly different when comparing either construct or when compared to WT $InsP_3R$-1 (see Fig. 3).

presented here includes the observations that under appropriate conditions, channel activity was absolutely dependent on the presence of functional $InsP_3R$-1 and of an $InsP_3R$ agonist. Moreover, mutation of the $InsP_3R$-1 pore also resulted in rational, predictable changes in the channel's conductance. In a similar vein, the absence of the enhancing effect of forskolin in $InsP_3R$-1 constructs with mutations in the PKA phosphorylation sites adds further weight to the contention that $InsP_3R$-1 is responsible for the conductance observed. Importantly, the PM $InsP_3R$-1 was also shown to be regulated by Ca^{2+} and ATP in a similar fashion to the receptor expressed in its conventional ER environment (Taylor & Laude, 2002; Bezprozvanny, 2005; Foskett *et al.* 2007).

The major goal of the study was to use these methodologies to study the effects of PKA phosphorylation on $InsP_3R$-1 channel gating. Specifically, we monitored activity following activation of adenylate cyclase or by using $InsP_3R$-1 constructs which have been engineered to be either PKA non-phosphorylatable or mimic phosphorylation (Wagner *et al.* 2003, 2004). These complimentary protocols clearly illustrate the power of the experimental system. In the former experiments, the measurement of PM $InsP_3R$-1 activity in the whole cell mode of the patch clamp technique allows the activation of endogenous PM signalling pathways resulting in PKA activation. The latter experiments, however, presented here, unambiguously reflect the *direct* effect of phosphorylation on the intrinsic channel properties. These effects would be predicted to be largely independent of phosphorylation of other PKA substrates or cell-type specific events such as targeting (Tu *et al.* 2004).

Formally, the augmentation of the cytoplasmic Ca^{2+} signal observed following PKA activation (Wagner *et al.*

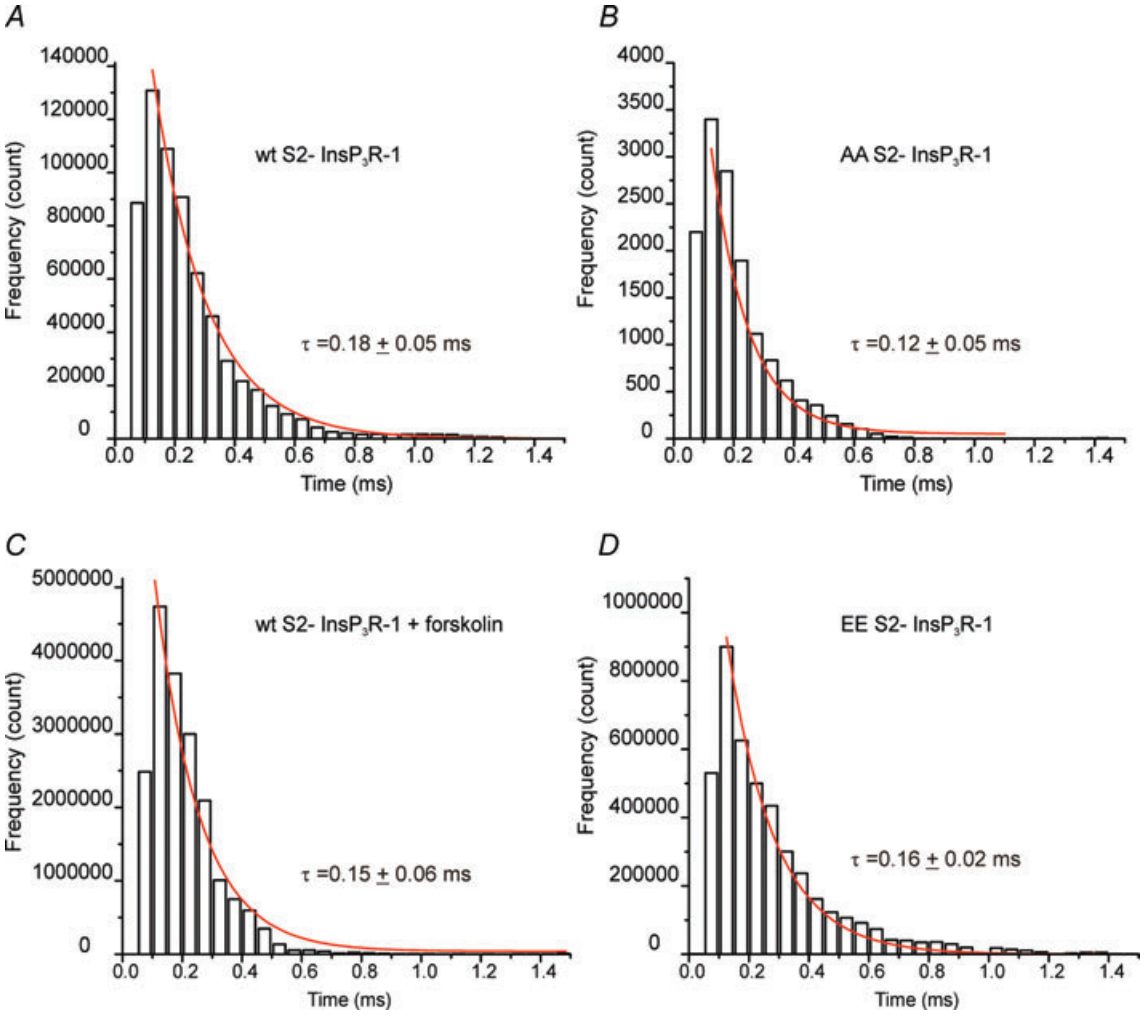

Figure 10. Distribution of $InsP_3R$-1 open dwell times during bursting activity
The open times were plotted for the indicated constructs/conditions and the distribution was fitted with a single exponential decay, shown in red. The τ was derived from this fit. *A*, WT $InsP_3R$-1. *B*, AA $InsP_3R$-1. *C*, WT $InsP_3R$-1 following addition of forskolin. *D*, EE $InsP_3R$-1. The τ derived under these various conditions was unaltered.

2003, 2004) could occur either by increased Ca^{2+} flux through individual receptors as a result of a larger single channel conductance (i_{Ca}) and/or increased P_o, or additionally by insertion/activation of previously silent channels. Under conditions when the channel could be considered phosphorylated (either following forskolin treatment or comparing AA to EE $InsP_3R$-1) the studies presented here reveal a marked increase in $InsP_3R$-1 P_o. No change in channel conductance or obvious recruitment of additional PM channels was observed. Specifically, phosphoregulation of the channel leads to a change in the principle $InsP_3R$-1 gating mode such that the increase in P_o occurs because the channel gates in 'bursts'. Bursting activity was characterized by periods when the channel rapidly transitions from open to the closed state followed by pronounced refractory periods. So-called 'modal gating' is also a characteristic of L-type voltage gated Ca^{2+} channels (Hess *et al.* 1984; Tsien *et al.* 1986; Yue *et al.* 1990) and phosphorylation by PKA or modulation by dihydropyridine agonists is reported to initiate a 'mode switch'. This is proposed to occur by reversibly stabilizing a particular conformation of the channel, thus favouring particular gating characteristics (Tsien *et al.* 1986; Yue *et al.* 1990). This mode of gating is also reminiscent of the predominant activity described at optimal Ca^{2+} and saturating [$InsP_3$] in a recent publication describing modal gating behaviour of nuclear Sf9 cell $InsP_3R$ (Ionescu *et al.* 2007) and is consistent with behaviour in the present study of the non-phosphorylated channel at higher [$InsP_3R$ agonist] (e.g. Fig. 7). Ionescu *et al.* (2007) have proposed that the $InsP_3R$ gates in three predominant modes: a low activity mode, a fast kinetic mode and a burst mode exhibiting high P_o. They suggest that because $InsP_3$ does not significantly alter the P_o of the channel

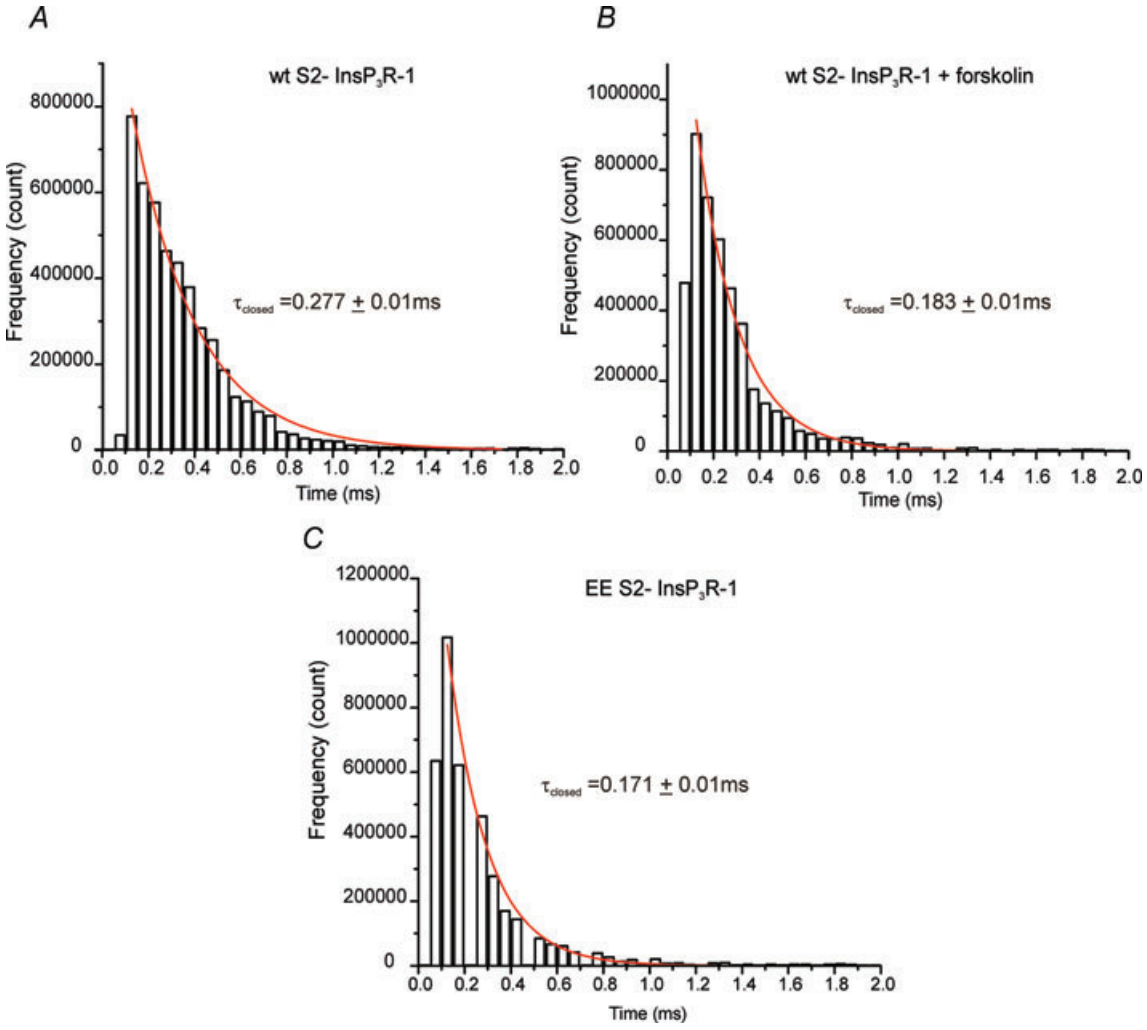

Figure 11. Distribution of $InsP_3R$-1 closed dwell times during bursting activity
The closed times were plotted for the indicated constructs/conditions and the distribution was fitted with a single exponential decay, shown in red. The τ was derived from this fit. *A*, WT $InsP_3R$-1. *B*, WT $InsP_3R$-1 following addition of forskolin. *C*, EE $InsP_3R$-1. Phosphorylation significantly shortened the τ, thus favouring channel opening.

in any particular mode, the principal effect of $InsP_3$ is to influence the amount of time the channel resides in a particular mode. Thus, as [$InsP_3$] increases, the likelihood that the channel is in the burst mode is higher and in low activity mode is lower. Because specialized algorithms were used to identify these gating modes and the recording conditions were different, we cannot unequivocally establish that our data are consistent with the presence of three distinct modes of channel activity and therefore consistent with this model. Nevertheless, at least superficially, PKA-induced phosphorylation of $InsP_3R$-1 appears to adhere to this paradigm, whereby the channel is exhibiting extended bursting characteristics typical of higher [$InsP_3$]. Kinetic analysis of the length of bursts and burst intervals, together with gating within the burst, reveals the biophysical basis for the mechanism underlying the effects of PKA phosphoregulation. The major effects of phosphorylation are to dramatically destabilize a long-lived closed state. To a lesser extent, phosphorylation also destabilizes a short-lived closed state and both events contribute to bursting activity ultimately resulting in enhanced Ca^{2+} release.

The increased P_o and bursting activity of the phosphorylated $InsP_3R$-1 are consistent with a shift in the functional affinity for $InsP_3$. No change in binding of $InsP_3$ *per se* was detected and thus phosphorylation does not directly affect the affinity of $InsP_3$ for its ligand. Many current models for the action of $InsP_3$ on $InsP_3R$ propose that binding ultimately gates the channel by shifting the Ca^{2+} sensitivity of the receptor. The current

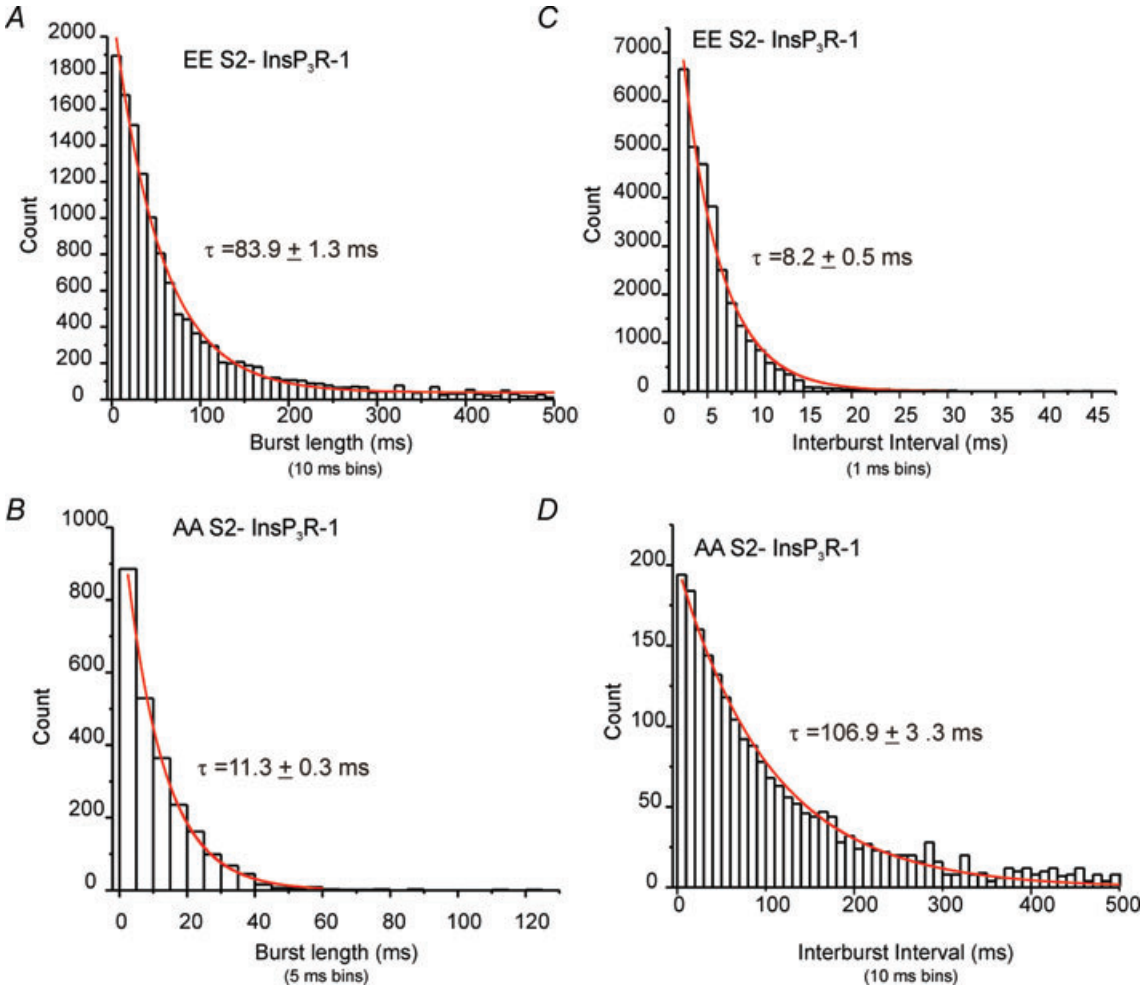

Figure 12. Distribution of $InsP_3R$-1 burst lengths and interburst intervals
Bursting activity was defined as described in Methods. *A*, the distribution and fit for this distribution of burst length duration for EE $InsP_3R$-1. *B*, a similar analysis for AA $InsP_3R$-1. The τ derived from these data indicates that phosphorylation decreases the rate of transition from an open-state to a long lived closed state. *C*, the distribution and fit of the duration of interburst intervals for EE $InsP_3R$-1. *D*, a similar analysis of AA $InsP_3R$-1 interburst intervals. The τ derived from these data indicates that phosphorylation further favours bursting activity by destabilizing a long lived closed state favouring channel opening.

models for the action of Ca^{2+} essentially state that there are two binding sites for Ca^{2+}, one inhibitory and a second which stimulates $InsP_3R$ activity (Mak *et al.* 2001, 2003; Taylor & Laude, 2002). $InsP_3$ binding to $InsP_3R$ then modulates the Ca^{2+} affinity of one or both of these sites such that channel opening and Ca^{2+} release is initially favoured. Because $InsP_3$ alters the affinity for Ca^{2+} and thereby its ability to reduce $InsP_3R$ P_o, without altering the affinity for the stimulatory effect, Foskett and colleagues have proposed that the primary effect of $InsP_3$ binding is to markedly reduce the affinity of the Ca^{2+} inhibitory site and thus favour activation of Ca^{2+} release (Mak *et al.* 2003; Foskett *et al.* 2007). On the basis of these ideas, it is somewhat surprising that the Ca^{2+} dependence of activation or inhibition of channel activity was essentially identical in AA and EE $InsP_3R$-1. These data suggests it is unlikely that PKA phosphorylation shifts the functional $InsP_3$ dependence in this manner. The question is then, how can phosphorylation lead to an increase in $InsP_3R$-1 P_o? PKA- induced phosphorylation (or phosphomimetic mutation) is thought to alter protein function as the net negative charge imparted by the addition of the phosphate group to the phosphoacceptor residue neutralizes the positive charge of an upstream basic arginine or lysine residue. This change in electrostatic character or hydrophobicity of this region of the protein could have numerous potential effects to influence $InsP_3R$-1 function. For example, a relatively direct effect might include a charge-induced conformational change, facilitating or stabilizing an intra-domain interaction which ultimately favours a bursting mode of channel gating similar to the mode-switching which occurs with L-type Ca^{2+} channels (Hess *et al.* 1984). A change in conformation or charge could conceivably also have less direct effects to alter the interactions with soluble cytosolic binding partners, such as adenine nucleotides or the large number of protein binding partners which modulate $InsP_3R$-1 activity. Indeed, although unlikely to explain the current data, PKA phosphorylation of $InsP_3R$-1 has been reported to alter the receptors association with calmodulin (Lin *et al.* 2000).

In conclusion, by analysis of $InsP_3R$-1 localized in the PM of DT40 cells, we demonstrate that PKA phosphorylation results in markedly enhanced single channel P_o without any effect on single channel conductance or the number of active channels. The increase in P_o is largely accomplished by a transition to channel bursting. Moreover, the techniques used here have great potential to facilitate further mechanistic study of the regulation of $InsP_3R$ at the single channel level.

References

Adkins CE, Wissing F, Potter BV & Taylor CW (2000). Rapid activation and partial inactivation of inositol trisphosphate receptors by adenophostin A. *Biochem J* **352**, 929–933.

Berridge MJ (1993). Inositol trisphosphate and calcium signalling. *Nature* **361**, 315–325.

Bezprozvanny I (2005). The inositol 1,4,5-trisphosphate receptors. *Cell Calcium* **38**, 261–272.

Bezprozvanny I & Ehrlich BE (1993). ATP modulates the function of inositol 1,4,5-trisphosphate-gated channels at two sites. *Neuron* **10**, 1175–1184.

Bezprozvanny I, Watras J & Ehrlich BE (1991). Bell-shaped calcium-response curves of $Ins(1,4,5)P_3$- and calcium-gated channels from endoplasmic reticulum of cerebellum. *Nature* **351**, 751–754.

Boehning D & Joseph SK (2000). Functional properties of recombinant type I and type III inositol 1,4,5-trisphosphate receptor isoforms expressed in COS-7 cells. *J Biol Chem* **275**, 21492–21499.

Boehning D, Mak DO, Foskett JK & Joseph SK (2001). Molecular determinants of ion permeation and selectivity in inositol 1,4,5-trisphosphate receptor Ca^{2+} channels. *J Biol Chem* **276**, 13509–13512.

Bruce JI, Shuttleworth TJ, Giovannucci DR & Yule DI (2002). Phosphorylation of inositol 1,4,5-trisphosphate receptors in parotid acinar cells. A mechanism for the synergistic effects of cAMP on Ca^{2+} signaling. *J Biol Chem* **277**, 1340–1348.

Bruce JI, Straub SV & Yule DI (2003). Crosstalk between cAMP and Ca^{2+} signaling in non-excitable cells. *Cell Calcium* **34**, 431–444.

Chaloux B, Caron AZ & Guillemette G (2007). Protein kinase A increases the binding affinity and the Ca^{2+} release activity of the inositol 1,4,5-trisphosphate receptor type 3 in RINm5F cells. *Biol Cell* **99**, 379–388.

Danoff SK, Ferris CD, Donath C, Fischer GA, Munemitsu S, Ullrich A, Snyder SH & Ross CA (1991). Inositol 1,4,5-trisphosphate receptors: distinct neuronal and nonneuronal forms derived by alternative splicing differ in phosphorylation. *Proc Natl Acad Sci U S A* **88**, 2951–2955.

Dellis O, Dedos SG, Tovey SC, Taufiq Ur R, Dubel SJ & Taylor CW (2006). Ca^{2+} entry through plasma membrane IP_3 receptors. *Science* **313**, 229–233.

Dellis O, Rossi AM, Dedos SG & Taylor CW (2008). Counting functional inositol 1,4,5-trisphosphate receptors into the plasma membrane. *J Biol Chem* **283**, 751–755.

Fadool DA & Ache BW (1992). Plasma membrane inositol 1,4,5-trisphosphate-activated channels mediate signal transduction in lobster olfactory receptor neurons. *Neuron* **9**, 907–918.

Finch EA, Turner TJ & Goldin SM (1991). Subsecond kinetics of inositol 1,4,5-trisphosphate-induced calcium release reveal rapid potentiation and subsequent inactivation by calcium. *Ann N Y Acad Sci* **635**, 400–403.

Foskett JK, White C, Cheung KH & Mak DO (2007). Inositol trisphosphate receptor Ca^{2+} release channels. *Physiol Rev* **87**, 593–658.

Furuichi T, Yoshikawa S, Miyawaki A, Wada K, Maeda N & Mikoshiba K (1989). Primary structure and functional expression of the inositol 1,4,5-trisphosphate-binding protein P400. *Nature* **342**, 32–38.

Galvan DL, Borrego-Diaz E, Perez PJ & Mignery GA (1999). Subunit oligomerization, and topology of the inositol 1,4,5-trisphosphate receptor. *J Biol Chem* **274**, 29483–29492.

Hess P, Lansman JB & Tsien RW (1984). Different modes of Ca channel gating behaviour favoured by dihydropyridine Ca agonists and antagonists. *Nature* **311**, 538–544.

Higo T, Hattori M, Nakamura T, Natsume T, Michikawa T & Mikoshiba K (2005). Subtype-specific and ER lumenal environment-dependent regulation of inositol 1,4,5-trisphosphate receptor type 1 by ERp44. *Cell* **120**, 85–98.

Iino M (1990). Biphasic Ca^{2+} dependence of inositol 1,4,5-trisphosphate-induced Ca release in smooth muscle cells of the guinea pig taenia caeci. *J Gen Physiol* **95**, 1103–1122.

Iino M (1991). Effects of adenine nucleotides on inositol 1,4,5-trisphosphate-induced calcium release in vascular smooth muscle cells. *J Gen Physiol* **98**, 681–698.

Ionescu L, Cheung KH, Vais H, Mak DO, White C & Foskett JK (2006). Graded recruitment and inactivation of single $InsP_3$ receptor Ca^{2+}-release channels: implications for quantal Ca^{2+} release. *J Physiol* **573**, 645–662.

Ionescu L, White C, Cheung KH, Shuai J, Parker I, Pearson JE, Foskett JK & Mak DO (2007). Mode switching is the major mechanism of ligand regulation of $InsP_3$ receptor calcium release channels. *J Gen Physiol* **130**, 631–645.

Iwai M, Tateishi Y, Hattori M, Mizutani A, Nakamura T, Futatsugi A, Inoue T, Furuichi T, Michikawa T & Mikoshiba K (2005). Molecular cloning of mouse type 2 and type 3 inositol 1,4,5-trisphosphate receptors and identification of a novel type 2 receptor splice variant. *J Biol Chem* **280**, 10305–10317.

Joseph SK, Bokkala S, Boehning D & Zeigler S (2000). Factors determining the composition of inositol trisphosphate receptor hetero-oligomers expressed in COS cells. *J Biol Chem* **275**, 16084–16090.

Kaur R, Zhu XO, Moorhouse AJ & Barry PH (2001). IP_3-gated channels and their occurrence relative to CNG channels in the soma and dendritic knob of rat olfactory receptor neurons. *J Membr Biol* **181**, 91–105.

Kuno M & Gardner P (1987). Ion channels activated by inositol 1,4,5-trisphosphate in plasma membrane of human T-lymphocytes. *Nature* **326**, 301–304.

Lange Y, Ye J, Rigney M & Steck TL (1999). Regulation of endoplasmic reticulum cholesterol by plasma membrane cholesterol. *J Lipid Res* **40**, 2264–2270.

Lin C, Widjaja J & Joseph SK (2000). The interaction of calmodulin with alternatively spliced isoforms of the type-I inositol trisphosphate receptor. *J Biol Chem* **275**, 2305–2311.

Maes K, Missiaen L, De Smet P, Vanlingen S, Callewaert G, Parys JB & De Smedt H (2000). Differential modulation of inositol 1,4,5-trisphosphate receptor type 1 and type 3 by ATP. *Cell Calcium* **27**, 257–267.

Maes K, Missiaen L, Parys JB, De Smet P, Sienaert I, Waelkens E, Callewaert G & De Smedt H (2001). Mapping of the ATP-binding sites on inositol 1,4,5-trisphosphate receptor type 1 and type 3 homotetramers by controlled proteolysis and photoaffinity labeling. *J Biol Chem* **276**, 3492–3497.

Mak DO & Foskett JK (1994). Single-channel inositol 1,4,5-trisphosphate receptor currents revealed by patch clamp of isolated *Xenopus* oocyte nuclei. *J Biol Chem* **269**, 29375–29378.

Mak DO & Foskett JK (1997). Single-channel kinetics, inactivation, and spatial distribution of inositol trisphosphate (IP_3) receptors in *Xenopus* oocyte nucleus. *J Gen Physiol* **109**, 571–587.

Mak DO, McBride S & Foskett JK (1999). ATP regulation of type 1 inositol 1,4,5-trisphosphate receptor channel gating by allosteric tuning of Ca^{2+} activation. *J Biol Chem* **274**, 22231–22237.

Mak DO, McBride S & Foskett JK (2001). Regulation by Ca^{2+} and inositol 1,4,5-trisphosphate ($InsP_3$) of single recombinant type 3 InsP3 receptor channels. Ca^{2+} activation uniquely distinguishes types 1 and 3 $InsP_3$ receptors. *J Gen Physiol* **117**, 435–446.

Mak DO, McBride SM, Petrenko NB & Foskett JK (2003). Novel regulation of calcium inhibition of the inositol 1,4,5-trisphosphate receptor calcium-release channel. *J Gen Physiol* **122**, 569–581.

Mak DO, McBride S, Raghuram V, Yue Y, Joseph SK & Foskett JK (2000). Single-channel properties in endoplasmic reticulum membrane of recombinant type 3 inositol trisphosphate receptor. *J Gen Physiol* **115**, 241–256.

Maranto AR (1994). Primary structure, ligand binding, and localization of the human type 3 inositol 1,4,5-trisphosphate receptor expressed in intestinal epithelium. *J Biol Chem* **269**, 1222–1230.

Nakagawa T, Okano H, Furuichi T, Aruga J & Mikoshiba K (1991). The subtypes of the mouse inositol 1,4,5-trisphosphate receptor are expressed in a tissue-specific and developmentally specific manner. *Proc Natl Acad Sci U S A* **88**, 6244–6248.

Parker AK, Gergely FV & Taylor CW (2004). Targeting of inositol 1,4,5-trisphosphate receptors to the endoplasmic reticulum by multiple signals within their transmembrane domains. *J Biol Chem* **279**, 23797–23805.

Patel S, Joseph SK & Thomas AP (1999). Molecular properties of inositol 1,4,5-trisphosphate receptors. *Cell Calcium* **25**, 247–264.

Ramos-Franco J, Caenepeel S, Fill M & Mignery G (1998*a*). Single channel function of recombinant type-1 inositol 1,4,5-trisphosphate receptor ligand binding domain splice variants. *Biophys J* **75**, 2783–2793.

Ramos-Franco J, Fill M & Mignery GA (1998*b*). Isoform-specific function of single inositol 1,4,5-trisphosphate receptor channels. *Biophys J* **75**, 834–839.

Ramos-Franco J, Galvan D, Mignery GA & Fill M (1999). Location of the permeation pathway in the recombinant type 1 inositol 1,4,5-trisphosphate receptor. *J Gen Physiol* **114**, 243–250.

Soulsby MD, Alzayady K, Xu Q & Wojcikiewicz RJ (2004). The contribution of serine residues 1588 and 1755 to phosphorylation of the type I inositol 1,4,5-trisphosphate receptor by PKA and PKG. *FEBS Lett* **557**, 181–184.

Stehno-Bittel L, Luckhoff A & Clapham DE (1995). Calcium release from the nucleus by $InsP_3$ receptor channels. *Neuron* **14**, 163–167.

Sudhof TC, Newton CL, Archer BT 3rd, Ushkaryov YA & Mignery GA (1991). Structure of a novel $InsP_3$ receptor. *EMBO J* **10**, 3199–3206.

Supattapone S, Danoff SK, Theibert A, Joseph SK, Steiner J & Snyder SH (1988*a*). Cyclic AMP-dependent phosphorylation of a brain inositol trisphosphate receptor decreases its release of calcium. *Proc Natl Acad Sci U S A* **85**, 8747–8750.

Supattapone S, Worley PF, Baraban JM & Snyder SH (1988*b*). Solubilization, purification, and characterization of an inositol trisphosphate receptor. *J Biol Chem* **263**, 1530–1534.

Tang TS, Tu H, Wang Z & Bezprozvanny I (2003). Modulation of type 1 inositol (1,4,5)-trisphosphate receptor function by protein kinase A and protein phosphatase 1a. *J Neurosci* **23**, 403–415.

Tanimura A, Tojyo Y & Turner RJ (2000). Evidence that type I, II, and III inositol 1,4,5-trisphosphate receptors can occur as integral plasma membrane proteins. *J Biol Chem* **275**, 27488–27493.

Taylor CW, Genazzani AA & Morris SA (1999). Expression of inositol trisphosphate receptors. *Cell Calcium* **26**, 237–251.

Taylor CW & Laude AJ (2002). IP_3 receptors and their regulation by calmodulin and cytosolic Ca^{2+}. *Cell Calcium* **32**, 321–334.

Thrower EC, Park HY, So SH, Yoo SH & Ehrlich BE (2002). Activation of the inositol 1,4,5-trisphosphate receptor by the calcium storage protein chromogranin A. *J Biol Chem* **277**, 15801–15806.

Tsien RW, Bean BP, Hess P, Lansman JB, Nilius B & Nowycky MC (1986). Mechanisms of calcium channel modulation by b-adrenergic agents and dihydropyridine calcium agonists. *J Mol Cellular Cardiol* **18**, 691–710.

Tu H, Tang TS, Wang Z & Bezprozvanny I (2004). Association of type 1 inositol 1,4,5-trisphosphate receptor with AKAP9 (Yotiao) and protein kinase A. *J Biol Chem* **279**, 19375–19382.

Vaca L & Kunze DL (1995). IP_3-activated Ca^{2+} channels in the plasma membrane of cultured vascular endothelial cells. *Am J Physiol Cell Physiol* **269**, C733–C738.

van Rossum DB, Patterson RL, Kiselyov K, Boehning D, Barrow RK, Gill DL & Snyder SH (2004). Agonist-induced Ca^{2+} entry determined by inositol 1,4,5-trisphosphate recognition. *Proc Natl Acad Sci U S A* **101**, 2323–2327.

Vazquez G, Wedel BJ, Bird GS, Joseph SK & Putney JW (2002). An inositol 1,4,5-trisphosphate receptor-dependent cation entry pathway in DT40 B lymphocytes. *EMBO J* **21**, 4531–4538.

Wagner LE 2nd, Betzenhauser MJ & Yule DI (2006). ATP binding to a unique site in the type-1, $S2^-$ inositol 1,4,5-trisphosphate receptor defines susceptibility to phosphorylation by protein kinase A. *J Biol Chem* **281**, 17410–17419.

Wagner LE 2nd, Li WH, Joseph SK & Yule DI (2004). Functional consequences of phosphomimetic mutations at key cAMP-dependent protein kinase phosphorylation sites in the type 1 inositol 1,4,5-trisphosphate receptor. *J Biol Chem* **279**, 46242–46252.

Wagner LE 2nd, Li WH & Yule DI (2003). Phosphorylation of type-1 inositol 1,4,5-trisphosphate receptors by cyclic nucleotide-dependent protein kinases: a mutational analysis of the functionally important sites in the $S2^+$ and $S2^-$ splice variants. *J Biol Chem* **278**, 45811–45817.

Walaas SI, Nairn AC & Greengard P (1983). Regional distribution of calcium- and cyclic adenosine 3′:5′-monophosphate-regulated protein phosphorylation systems in mammalian brain. I. Particulate systems. *J Neurosci* **3**, 291–301.

Walaas SI, Nairn AC & Greengard P (1986). PCPP-260, a Purkinje cell-specific cyclic AMP-regulated membrane phosphoprotein of M_r 260,000. *J Neurosci* **6**, 954–961.

Wojcikiewicz RJ (1995). Type I, II, and III inositol 1,4,5-trisphosphate receptors are unequally susceptible to down-regulation and are expressed in markedly different proportions in different cell types. *J Biol Chem* **270**, 11678–11683.

Wojcikiewicz RJ & Luo SG (1998). Phosphorylation of inositol 1,4,5-trisphosphate receptors by cAMP-dependent protein kinase. Type I, II, and III receptors are differentially susceptible to phosphorylation and are phosphorylated in intact cells. *J Biol Chem* **273**, 5670–5677.

Yoshikawa F, Morita M, Monkawa T, Michikawa T, Furuichi T & Mikoshiba K (1996). Mutational analysis of the ligand binding site of the inositol 1,4,5-trisphosphate receptor. *J Biol Chem* **271**, 18277–18284.

Yue DT, Herzig S & Marban E (1990). β-Adrenergic stimulation of calcium channels occurs by potentiation of high-activity gating modes. *Proc Natl Acad Sci U S A* **87**, 753–757.

Acknowledgements

The Authors are very grateful to Ted Begenisich for the insight and helpful discussion regarding the single channel analysis. The Authors would also like to thank Dr James Sneyd and Elan Gin for discussion of the single channel analysis, Dr Trevor Shuttleworth and Matt Betzenhauser for critical reading of the manuscript and Lyndee Bilodeau for invaluable technical support. This work was supported by NIH grants DK54568 and DE14756 (D.I.Y.) and DK34804 (S.K.J.).

Supplemental material

Online supplemental material for this paper can be accessed at:
http://jp.physoc.org/cgi/content/full/jphysiol.2008.152314/DC1
and
http://www.blackwell-synergy.com/doi/suppl/10.1113/jphysiol.2008.152314